LASER-INDUCED POPULATION TRANSFER BY ADIABATIC PASSAGE TECHNIQUES

Nikolay V Vitanov[1], Thomas Halfmann[2], Bruce W Shore[3], and Klaas Bergmann[2]

[1]*Helsinki Institute of Physics, PL 9, 00014 University of Helsinki, Finland*
e-mail: nikolay.vitanov@helsinki.fi
[2]*Fachbereich Physik, Universität Kaiserslautern, 67653 Kaiserslautern, Germany*
[3]*Lawrence Livermore National Laboratory, Livermore, California 94550*

Key Words stimulated Raman adiabatic passage, level crossing, coherent excitation, Landau-Zener model

■ **Abstract** We review some basic techniques for laser-induced adiabatic population transfer between discrete quantum states in atoms and molecules.

1. INTRODUCTION

Atoms and molecules prepared in well-defined quantum states are instrumental in modern atomic and molecular physics, not only in traditional studies of state-to-state collision dynamics or laser-controlled chemical reactions, but also in various new areas, e.g. atom optics and quantum information. The development of efficient schemes for selective population transfer, such as chirped-pulse excitation and stimulated Raman adiabatic passage (STIRAP), have opened new opportunities for coherent laser control of atomic and molecular processes. This article overviews a variety of techniques, with associated theory, whereby one can accomplish complete population transfer in atoms and molecules by means of adiabatic time evolution induced by properly crafted laser pulses.

The central idea of population transfer is to begin with an atom or molecule in which the internal structure is in a specified discrete quantum state and then, by exposing this system to a controlled pulse of radiation, force the internal structure into a desired target state. Only a radiation field, suitably monochromatized and near-resonant with the atomic Bohr frequency, can provide the selectivity needed to isolate a single final state. A goal of theory is to predict, for a specified set of

---

[1]Also at Department of Physics, Sofia University, James Boucher 5 Blvd., 1126 Sofia, Bulgaria and Institute of Solid State Physics, Bulgarian Academy of Sciences, Tzarigradsko shaussee 72, 1784 Sofia, Bulgaria.

radiation pulses, the probability that atoms will undergo a transition between the initial state and the desired target state. Alternatively, theory should provide a prescription for pulses that will produce a desired population transfer.

The population transfer techniques described in this review have in common the need for coherent laser radiation. To emphasize the qualitative importance of coherence in the radiation field, we first summarize some basic results obtainable with incoherent light, such as that from filtered atomic vapor lamps or from broadband lasers with poor coherence properties.

1.1 Incoherent Population Transfer Schemes

1.1.1 Incoherent Excitation of Two-State Systems   One of the simplest theoretical descriptions of near-resonant excitation of a two-state atom or molecule by incoherent radiation is credited to Einstein, who first postulated that the rate of change in an atomic population within a blackbody cavity is proportional to radiation energy density (1); the Einstein B coefficient quantifies this proportionality. The resulting rate equations (cf (2); Section 2.2) include not only transitions induced by any experimentally controlled radiation field, but also the possibility of spontaneous emission of radiation, as quantified by the Einstein A coefficient ($1/A$ is the spontaneous emission lifetime). If the atoms are initially (at time $t \rightarrow -\infty$) unexcited, if the radiation is sufficiently intense that spontaneous emission has a negligible effect on the population (the saturated regime), and if the excited level has the same degeneracy as the initial level, then the excited-state population at time t is

$$P_e(t) = \frac{1}{2}[1 - e^{-BF(t)}], \qquad \qquad 1.$$

where $F(t) = \int_{-\infty}^{t} I(t')dt'$ is the pulsed radiation fluence (energy per unit area) up to time t, $I(t)$ being the time-varying laser intensity (power per unit area). As this expression shows, when the pulse fluence increases, the excited-state population approaches monotonically the saturation value of 50%, which is the best transfer efficiency one can achieve with incoherent light. Of course, once the radiation ceases, the atom must return to lower-lying levels by spontaneously emitting radiation, and eventually no excitation will remain.

1.1.2 Optical Pumping   Although spontaneous emission hinders direct creation of excitation, it can be used to advantage. Consider the excitation linkage shown in Figure 1*a*: an initially populated state ψ_1, resonantly excited to state ψ_2, from which spontaneous emission occurs, not only returning to state ψ_1 but possibly also to some third state ψ_3 whose energy lies far from resonance with the initial state or which is prevented, by selection rules based on polarization of the light, from being excited by the intense radiation. Every time the atom is excited from state ψ_1 to state ψ_2 by absorbing a photon there is a chance that spontaneous emission will carry the population to state ψ_3, after which the atom will be immune to further action by the radiation. The resulting population transfer, optical pumping, will eventually place the entire population into state ψ_3.
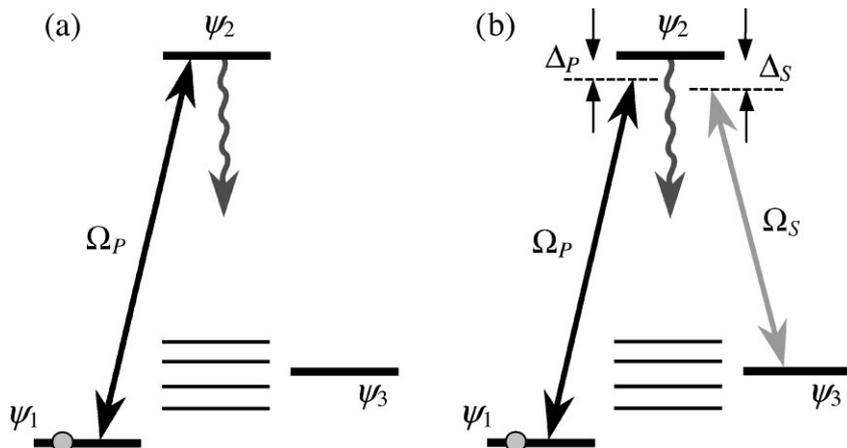
Figure 1 (*a*) Linkage diagram for optical pumping. A pump field (not necessarily a laser) excites state ϕ_2, which spontaneously decays back to state ϕ_1, to state ϕ_3, or possibly to some other states. (*b*) Linkage diagram for stimulated emission pumping. A pump field populates state ϕ_2, and a subsequent Stokes (or dump) field populates state ϕ_3.

The simplicity of optical pumping, which requires only a single light source (not necessarily a laser), has made it a widely used method for preparing atoms or molecules in a well-defined ground or metastable state. Its main limitation is the lack of selectivity: Because the population arrives in the target level by spontaneous emission, it will simultaneously arrive in all levels into which the excited state can decay. Therefore, the pumping procedure will generally populate a statistical mixture of possible final states, not a single state. The distribution of final populations is determined by the relative decay rates that link each final state with the excited state. For vibrational transitions, these rates are proportional to Franck-Condon factors; because the latter rarely exceed 10%, the selectivity is correspondingly low.

1.1.3 Stimulated Emission Pumping   Optical pumping uses only a single light source, acting on the pump transition. The overall transfer, however, involves two photons: absorption of a pump photon from the imposed light source and spontaneous emission of a Stokes photon. The names pump and Stokes serve notice that we are dealing with a two-photon Raman process. It is natural to consider a Raman-type process in which both fields are externally supplied (a stimulated Raman process), so that the final step proceeds to a selected final state rather than to a statistical distribution.

One variant of the suggested two-photon process of population transfer, stimulated emission pumping (SEP) (2), uses a pump field to place a population from the initial state ψ_1 into the excited state ψ_2, followed some time later by a Stokes (or dump) field that transfers the population into the desired final state ψ_3 (hence

the names pump and dump), as depicted by the Λ-type linkage in Figure 1*b*. If the intensity of the pump laser is sufficiently strong to saturate the $\psi_1 \leftrightarrow \psi_2$ transition, then, as suggested by the rate equations, the pump step can transfer at most 50% of the population from state ψ_1 to state ψ_2. If the Stokes laser is also sufficiently strong to saturate its transition, then half the population in state ψ_2 will be further transferred to the target state ψ_3. Hence, at most one quarter of the population is transferred to the target state, while one half of the population remains in the initial state. The remaining quarter is distributed statistically according to the branching of spontaneous emission from state ψ_2. The SEP efficiency can be improved slightly if the pump and Stokes pulses are applied simultaneously, rather than successively. If they are sufficiently strong to saturate the transitions, thereby equalizing the populations, then one third of the population can be dispatched to ψ_3.

Because of its simplicity, the SEP technique has enjoyed widespread application in collision dynamics and spectroscopy (3, 4). Its main limitations are low efficiency and low selectivity. Typically, a transfer efficiency of 10% is rarely exceeded, but this is quite adequate for many spectroscopic studies.

1.2   Resonant Coherent Excitation: Rabi Oscillations

The response of a quantum system to coherent (laser) radiation differs in significant and qualitative ways from the response of the same system to light from a lamp, even a very monochromatic lamp. Whereas the sudden application of incoherent radiation to an atom or molecule typically results in a monotonic approach to some equilibrium excitation, the sudden application of steady laser radiation typically produces oscillatory populations. These differences are most clearly seen in the study of two-state systems.

1.2.1 Two-State Systems   When coherent radiation is resonant (the carrier frequency equal to the Bohr frequency) and steady, the excitation oscillates sinusoidally (a behavior known as Rabi oscillations),

$$P_e(t) = \tfrac{1}{2}(1 - \cos \Omega t). \qquad\qquad 2.$$

The frequency of population oscillation Ω is known as the Rabi frequency; it will be associated below with the strength of the interaction. When the radiation varies in amplitude, the cosine argument is replaced by the so-called pulse area $A(t)$,

$$\Omega t \rightarrow \int_{-\infty}^{t} \Omega(t')dt' = A(t). \qquad\qquad 3.$$

Unlike the monotonic behavior for incoherent excitation, here the excited-state population oscillates between 0 and 1, depending on the value of $A(t)$. For pulse areas equal to odd multiples of π (odd-π pulses), a complete population transfer to the excited state takes place, whereas for pulse areas equal to even multiples of π (even-π pulses), the system returns to the initial state.

In practice, the sample of atoms or molecules consists of an ensemble, often with a distribution of velocities. Atoms moving in the direction of a traveling wave experience a Doppler shift, so that their excitation is not exactly resonant; their population oscillations are more rapid and have smaller peak values than those of resonant atoms. Atoms moving transversely to a laser beam will experience a pulse area dependent on the duration of their transit time across the beam. These velocity-dependent interactions and the presence of fluctuations in the laser intensity require an averaging over excitation probabilities. The result is an effective excitation probability that has less pronounced oscillations; in extreme cases the averaging can bring the excitation probability to 0.5, the same as with incoherent excitation.

1.2.2 Three-State Systems   Rabi cycling is not confined to two-state systems: It can be found in multi-state systems too. One example is a coherently driven three-state system subjected to the same pulse sequence as in SEP: the pump pulse first, followed after its completion (without overlap) by the Stokes pulse. Then the excitation can still be considered as a two-step process, but the probabilities for each step are different from those in SEP. In the case of exact single-photon resonances, the transition probabilities P_{12} from state ψ_1 to state ψ_2 and P_{23} from state ψ_2 to state ψ_3 are

$$P_{12} = \tfrac{1}{2}(1 - \cos A_P), \quad P_{23} = \tfrac{1}{2}(1 - \cos A_S), \qquad\qquad 4.$$

where A_P and A_S are the pump and Stokes pulse areas. If the system is initially in state ψ_1, then the population of state ψ_3 after the excitation is the product of the two probabilities,

$$P_{13} = \tfrac{1}{4}(1 - \cos A_P)(1 - \cos A_S). \qquad\qquad 5.$$

Hence, for suitably chosen pulse areas (both equal to odd multiples of π) there is complete population transfer from state ψ_1 to state ψ_3. However, the transfer efficiency depends strongly on the pulse areas, and it can even vanish (when A_P or A_S are even multiples of π).

When the pump and Stokes pulses have the same time dependence, the interaction dynamics can no longer be separated into two consecutive, independent two-state transitions. However, an exact solution can still be derived. If the system is initially in state ψ_1, and the two lasers are each resonantly tuned, then the population of state ψ_3 at the end of the excitation is

$$P_{13} = \frac{A_P A_S}{A^2}(1 - \cos \tfrac{1}{2}A), \qquad\qquad 6.$$

where $A = \sqrt{A_P^2 + A_S^2}$. Here again the transfer efficiency depends on the pulse areas: Complete population transfer from state ψ_1 to state ψ_3 occurs when $A = 2(2k + 1)\pi$ $(k = 0, 1, 2, \ldots)$ and $A_P = A_S$, whereas complete population return to the initial state ψ_1 takes place when $A = 4k\pi$.

As for two-state Rabi oscillations, the presence of a distribution of velocities or intensity fluctuations will tend to average out the oscillations and to lower the transfer efficiency. Moreover, because the population passes through the intermediate state ψ_2, inevitable population losses will take place by spontaneous emission unless the excitation time is much shorter than the lifetime of ψ_2.

The Rabi cycling is but one of the ways in which coherent laser pulses can induce population changes. Another class of change, adiabatic evolution, which is the focus of this review, can occur when the Hamiltonian changes slowly. The next section describes the basic principles of adiabatic population transfer by using a level crossing, and the following section describes adiabatic population transfer by sequential laser pulses.

2. ADIABATIC POPULATION TRANSFER VIA A LEVEL CROSSING

2.1 Two-State Systems

2.1.1 Coherent Excitation   For coherent laser excitation the correct description of the interaction dynamics is provided by the time-dependent Schrödinger equation (2),

$$i\hbar \frac{d}{dt}\mathbf{C}(t) = \mathsf{H}(t)\mathbf{C}(t). \qquad\qquad 7.$$

$\mathbf{C}(t) = [C_1(t), C_2(t)]^T$ is a column vector whose elements are the (complex-valued) probability amplitudes of the two states ψ_1 and ψ_2, and $\mathsf{H}(t)$ is the Hamiltonian of the atom-radiation system. The diagonal elements of $\mathsf{H}(t)$ are the energies of the two states E_1 and E_2, and the off-diagonal elements contain the laser-atom dipole interaction energy. Because the populations $P_n(t) = |C_n(t)|^2$ depend only on the magnitudes of the probability amplitudes, there is some leeway in choosing their phases. It proves particularly convenient to incorporate the state energies as phases. Then the off-diagonal element of the Hamiltonian matrix, which is proportional to the sinusoidally oscillating laser electric field, is multiplied by a phase factor oscillating at the Bohr transition frequency $\omega_0 = (E_2 - E_1)/\hbar$. Because the laser frequency ω is equal or very close to the transition frequency ω_0, the off-diagonal Hamiltonian element can be represented as a sum of two terms: one term oscillating rapidly at nearly twice the transition frequency $(\omega_0 + \omega)$ and another term oscillating slowly at frequency $\Delta = \omega_0 - \omega$, the atom-laser detuning. Unless the laser pulse is very short (e.g. a femtosecond pulse) or very intense, the rapidly oscillating term can be neglected; this is known as the rotating-wave approximation (RWA). When this is done, the Hamiltonian reads (2)

$$\mathsf{H}(t) = \hbar \begin{bmatrix} 0 & \frac{1}{2}\Omega(t) \\ \frac{1}{2}\Omega(t) & \Delta(t) \end{bmatrix}. \qquad\qquad 8.$$

The off-diagonal element $\Omega(t)$, known as the Rabi frequency, parameterizes the strength of the atom-laser interaction; it is proportional to the atomic transition

dipole moment $\mathbf{d}_{12}$ and the laser electric field amplitude $\mathcal{E}(t)$, i.e. $\Omega(t) = \mathbf{d}_{12} \cdot \mathcal{E}(t)/\hbar$. We assume for simplicity and without loss of generality that $\Omega(t)$ is real-valued and positive [its phase can always be attached to one of the probability amplitudes (2)]. The diagonal elements of H(t) are the two RWA energies: The zero element is the energy of state ψ_1 lifted (dressed) by the photon energy $\hbar\omega$ and used as the reference energy level, and Δ is the frequency offset (detuning) of state ψ_2.

2.1.2 Adiabatic States and Adiabatic Following   Theoretical discussion of time-evolving quantum systems is greatly facilitated by introducing a special coordinate system in the abstract space in which the state vector $\Psi(t)$ moves. The basis vectors in this moving coordinate system are the instantaneous eigen states $\Phi_k(t)$ of the Hamiltonian H(t)—the adiabatic states. These states are time-dependent superpositions of the unperturbed states ψ_1 and ψ_2 (also known as the diabatic states) (2),

$$\Phi_+(t) = \psi_1 \sin\Theta(t) + \psi_2 \cos\Theta(t), \qquad 9.$$

$$\Phi_-(t) = \psi_1 \cos\Theta(t) - \psi_2 \sin\Theta(t), \qquad 10.$$

where the mixing angle $\Theta(t)$ is defined (modulo π) as $\Theta(t) = \frac{1}{2}\arctan[\Omega(t)/\Delta(t)]$. The energies of the adiabatic states are the two eigenvalues of H(t),

$$\hbar\varepsilon_\pm(t) = \tfrac{1}{2}\hbar\left[\Delta(t) \pm \sqrt{\Delta^2(t) + \Omega^2(t)}\right]. \qquad 11.$$

When the evolution is adiabatic no transitions between the adiabatic states occur. Mathematically, adiabatic evolution requires that the coupling between the adiabatic states is negligible compared with the difference between their eigen frequencies (2, 5, 6), i.e.,

$$|\langle\dot{\Phi}_+|\Phi_-\rangle| \ll |\varepsilon_+ - \varepsilon_-|, \qquad 12.$$

where the dot denotes a time derivative. Explicitly, the two-state adiabatic condition reads

$$\tfrac{1}{2}\left|\dot{\Omega}\Delta - \Omega\dot{\Delta}\right| \ll (\Omega^2 + \Delta^2)^{3/2}. \qquad 13.$$

Hence, adiabatic evolution requires a smooth pulse, long interaction time, and large Rabi frequency and/or large detuning. When the adiabatic condition holds there are no transitions between the adiabatic states, and their populations are conserved. In particular, if the system state vector $\Psi(t)$ coincides with a single adiabatic state $\Phi(t)$ at some time t, then it will remain in that adiabatic state as long as the evolution is adiabatic: The state vector $\Psi(t)$ will adiabatically follow the adiabatic state $\Phi(t)$. Of course, the relationship of the single adiabatic state $\Phi(t)$ to the diabatic states will change if the mixing angle $\Theta(t)$ changes, and so adiabatic evolution can produce population transfer between those diabatic states.

2.1.3 Rapid Adiabatic Passage   There are two distinct types of adiabatic population changes depending on the behavior of the diabatic energies 0 and $\hbar\Delta(t)$ of the Hamiltonians. The no-crossing case is depicted in Figure 2 (*top left frame*) in the particular case of constant detuning; the diabatic energies are parallel to each other. In the absence of interaction, the adiabatic energies coincide with the diabatic ones, but the (pulsed) interaction $\Omega(t)$ pushes them away from each other. As Equation 9 and 10 show, at early and late times each adiabatic state is identified with the same diabatic state: $\Phi_-(t \to \pm\infty) = \psi_1$, $\Phi_+(t \to \pm\infty) = \psi_2$, whereas at intermediate times it is a superposition of diabatic states. Consequently, starting from the ground state ψ_1, the population makes a partial excursion into the excited state ψ_2 at intermediate times and eventually returns to ψ_1 in the end (bottom left frame). Hence, in the no-crossing case adiabatic evolution leads to complete population return.

A rather different situation occurs when the detuning $\Delta(t)$ sweeps slowly from some very large negative value to some very large positive value (or vice versa), as shown in Figure 2 (*top right frame*). That is, the Hamiltonian at the end of
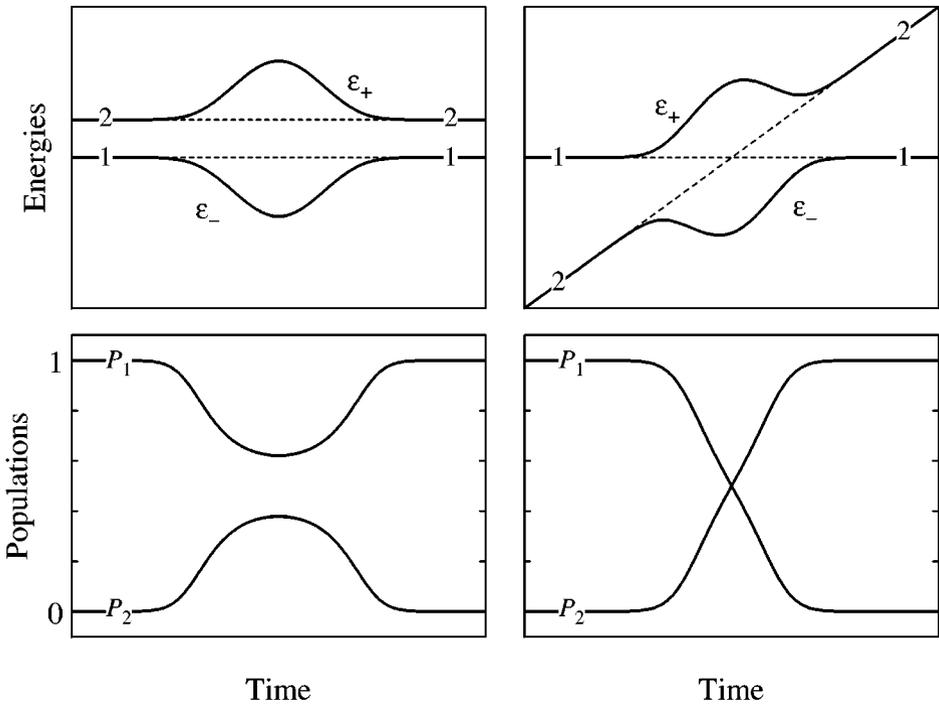
Figure 2   Time evolution of the energies (*upper frames*) and the populations (*lower frames*) in a two-state system. In the upper plots, the dashed lines show the unperturbed (diabatic) energies, and the solid curves show the adiabatic energies. The *left-hand frames* are for the no-crossing case, and the *right-hand frames* are for the level-crossing case.

the pulse differs from the Hamiltonian at the beginning because of the detuning change. Large in this context means much larger than the Rabi frequency $\Omega(t)$. The two diabatic energies 0 and $\hbar\Delta(t)$ intersect at time t_0 when the detuning is zero. The adiabatic energies approach the diabatic energies when $\Delta(t)$ is large (at early and late times), but the presence of interaction prevents their intersection—the adiabatic energies have an avoided crossing. Indeed, as Equation 10 shows, the eigen energy splitting $\hbar\varepsilon_+(t) - \hbar\varepsilon_-(t) = \hbar\sqrt{\Delta^2(t) + \Omega^2(t)}$ is equal to $\hbar\Omega(t_0)$ at the crossing. For constant $\Omega(t)$, this is the minimum value of the splitting, whereas for pulse-shaped $\Omega(t)$ (as in Figure 2), there are two minima near t_0. At extremely early and late times the ratio $\Delta(t)/\Omega(t) \xrightarrow{t\to\pm\infty} \pm\infty$. Hence, during the excitation the mixing angle $\Theta(t)$ rotates clockwise from $\Theta(-\infty) = \pi/2$ to $\Theta(+\infty) = 0$, and the composition of the adiabatic states changes accordingly. Asymptotically, each adiabatic state becomes uniquely identified with a single unperturbed state,

$$\psi_1 \xrightarrow{-\infty\leftarrow t} \Phi_+(t) \xrightarrow{t\to+\infty} \psi_2, \qquad\qquad 14.$$

$$-\psi_2 \xleftarrow{-\infty\leftarrow t} \Phi_-(t) \xleftarrow{t\to+\infty} \psi_1. \qquad\qquad 15.$$

Consequently, starting from state ψ_1, the system follows adiabatically the adiabatic state $\Phi_+(t)$ and eventually ends up in state ψ_2. The laser pulse, with detuning sweep, has produced complete population transfer, a process known as adiabatic passage or, because it must occur in a time shorter than the radiative lifetime of the excited state, as rapid adiabatic passage. We emphasize that adiabatic passage in a two-state system does not depend on the sign of the detuning slope: It takes place for both $\dot\Delta(t) > 0$ (as was assumed above) and $\dot\Delta(t) < 0$.

Adiabatic passage offers significant advantages over Rabi cycling as a means of producing complete population transfer in an ensemble of atoms. Unlike Rabi cycling, adiabatic passage is robust against small-to-moderate variations in the laser intensity, detuning, and interaction time. Therefore, it can produce uniform excitation for a broad range of Doppler shifts.

2.1.4 Estimating Transition Probabilities   A popular tool for estimating the transition probability between two crossing diabatic states is the Landau-Zener formula (7, 8),

$$P = 1 - p, \quad p = \exp\left[-\frac{\pi\Omega^2(t_0)}{2|\dot\Delta(t_0)|}\right], \qquad\qquad 16.$$

where $\dot\Delta(t_0)$ is the rate of change in the detuning evaluated at the crossing time t_0 and $\Omega(t_0)$ is the value of the Rabi frequency at t_0. This formula is exact only for a constant Rabi frequency and a linearly varying detuning over an infinite time interval, so it is only an approximation to any actual adiabatic passage. Nevertheless, it correctly identifies the importance of the ratio of Ω^2 to $\dot\Delta$ as a measure of the likelihood of population transfer. We note here that the probability for (nonadiabatic) transition between the adiabatic states is $p = 1 - P$.

There exist other, more realistic, models of level-crossing excitation. The Allen-Eberly-Hioe model (9, 10) assumes a hyperbolic-secant pulse and a hyperbolic-tangent chirp. The Demkov-Kunike model (11, 12) adds a static detuning to this model.

2.1.5 Experimental Demonstration   Population transfer by means of adiabatic passage was first used in nuclear magnetic resonance (13, 14), where the diabatic energies include interactions between nuclear magnetic moments and a magnetic field. The needed diabatic energy crossings are created by slowly changing either the frequency or the direction of an oscillating magnetic field.

Implementation of adiabatic passage in the optical region was suggested in the late 1960s (15). The process was demonstrated in the 1970s, during the early days of the application of laser radiation in atomic and molecular physics, with both one-photon (16–19) and two-photon transitions (20–22). The first demonstration of adiabatic following in laser excitation was achieved by Loy (16) in NH_3 with a fixed-frequency infrared laser; in this work a level crossing was created by Stark-shifting the transition frequency. Hamadani et al (23) observed adiabatic following in NH_3 by sweeping the laser frequency through resonance.

In the near infrared, adiabatic passage was observed by Avrillier et al (24) and Adam et al (25) [see also (26)], whereas Kroon et al (27) and Lorent et al (28) reported adiabatic following with visible light. In these experiments an atomic or molecular beam crossed a focused laser beam at right angles. If the molecules crossed the laser beam near its center, oscillations were observed in the excited-state population as the pulse area changed, as a result of either changing laser intensity (25) or changing time of flight (27). However, if the laser beam was focused off the molecular-beam axis, then the molecules experienced a curved wave front, which appeared to them as a time-varying Doppler shift (24, 25, 27). The detuning from resonance in this case was $\Delta(t) = v^2 \omega t / cr$, v being the longitudinal molecular velocity and r the wave front curvature. This effective chirp enabled adiabatic passage.

Various techniques are currently available for imposing a controlled frequency chirp on the laser field itself. Active electrooptic or acoustooptic modulation techniques provide straightforward means for sweeping the frequency of pulsed radiation with pulse length exceeding a microsecond. It is also straightforward to impose a frequency chirp on picosecond and femtosecond pulses (29–38). The large bandwidth of such ultrashort pulses allows spatial dispersion of the spectrum and subsequent time-delayed spatial recombination of the various frequency components. For example, adiabatic passage has been demonstrated by using picosecond pulses chirped by reflecting them off a suitably arranged pair of parallel gratings, tilted with respect to each other (39–49). The first grating separates the frequency components spatially, and the second one recombines them into a parallel beam. Because the optical path length between the gratings is frequency dependent, a chirp dependent on the path difference is generated. Such a setup

can provide an almost-linear frequency chirp. Self-phase modulation (29, 30, 50) is another technique for frequency chirping of picosecond pulses. For femtosecond pulses it suffices to propagate the laser beam through dispersive material, e.g. a thin molecular jet or a prism. For longer pulses a short length of optical fiber can be used (51). The self-phase modulation usually induces a phase shift $\varphi(t)$ proportional to the laser intensity, i.e. to $\Omega^2(t)$ (29, 30, 50). Hence, the detuning, which is proportional to $d\varphi(t)/dt$ (and therefore vanishes at early and late times), crosses resonance at the time when $\Omega(t)$ is maximum.

2.2 Stark-Chirped Rapid Adiabatic Passage

Techniques for producing frequency-swept pulses are not well developed for laser pulses of nanosecond duration. Nanosecond laser systems are used for many applications because they provide a very good combination of sufficiently high intensity (and hence large interaction strength) as well as long interaction time. The successful implementation of adiabatic evolution of laser-matter interaction relies on a combination of both parameters. Laser frequency chirping by active phase modulation, although possible in principle, is difficult for nanosecond laser pulses because it requires driving modulators at GHz frequencies. Alternatively, the spectral bandwidth of nanosecond pulses is too small for successful application of the techniques based on spatial dispersion that are well developed for femtosecond pulses. It appears feasible, however, to use laser-induced Stark shifts to modify the transition frequency.

2.2.1 Theory   It has been demonstrated recently (52, 53) that laser-induced Stark shifts can be used as a powerful tool for achieving efficient population transfer in two-state systems. This technique— Stark-chirped rapid adiabatic passage (SCRAP)—utilizes two sequential laser pulses. Figure 3 illustrates these ideas. One of the pulses—the pump pulse—is slightly detuned off resonance with the transition frequency and moderately strong; it serves to drive the population from the ground to the excited state. The other pulse—the Stark pulse—is far off-resonant and strong; it is used merely to modify the atomic transition frequency by inducing Stark shifts in the energies of the two states. Because the Stark shifts $S_g(t)$ and $S_e(t)$ of the ground and excited states are generally different (usually $|S_e(t)| \gg |S_g(t)|$) and each of them is proportional to the intensity of the Stark pulse, the transition frequency will experience a net Stark shift $S(t) = S_e(t) - S_g(t)$. By choosing an appropriate detuning for the pump pulse it is always possible to create two diabatic level crossings in the wings of the Stark pulse: one crossing during the growth and the other during the decline of the Stark pulse. For successful population transfer, the evolution must be adiabatic at one and only one of these crossings. This asymmetry can only occur if the pump and Stark pulses are not simultaneous: The pump pulse must be strong at one and only one of the crossings. It proves appropriate to set the time delay between the two pulses so that the maximum of the pump pulse occurs at one of the crossings in order to optimize the adiabatic passage there. It
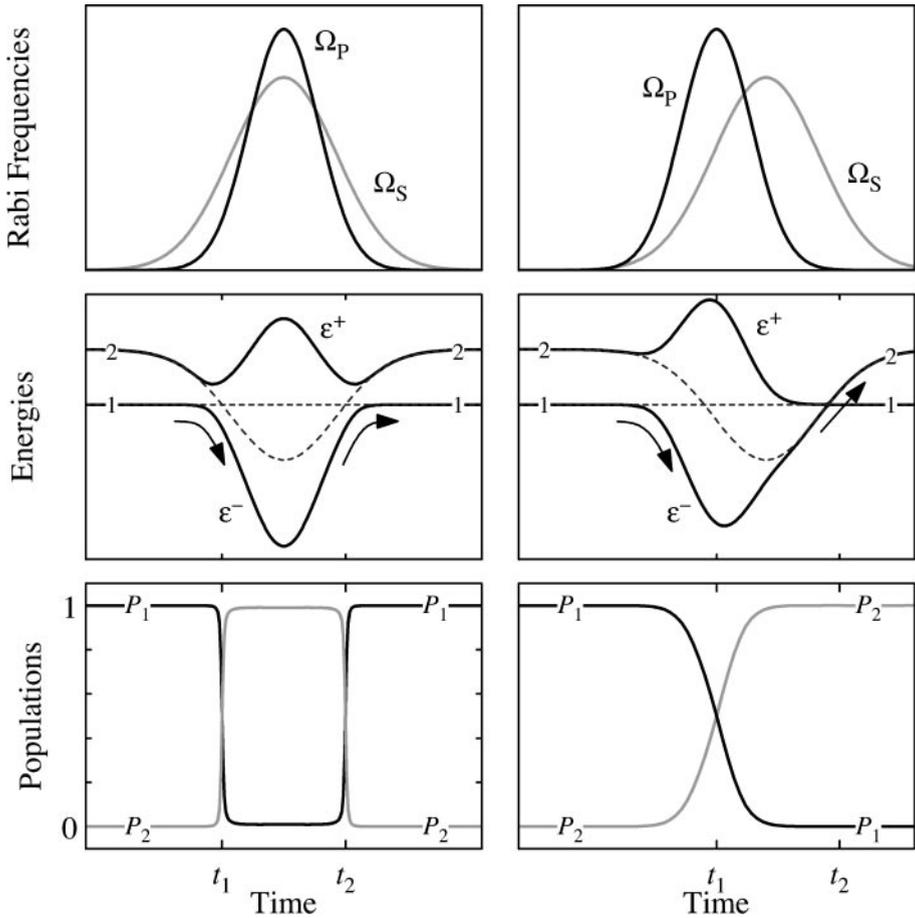
Figure 3   Time evolution of the Rabi frequencies (*top frames*), the level energies (*middle frames*), and the populations (*bottom frames*) in a two-state system driven by a pump pulse Ω_P and a Stark-shifting pulse Ω_S. (*Left*) Simultaneous pump and Stark pulses. (*Right*) Pump pulse before Stark pulse (Stark-chirped rapid adiabatic passage method).

is also appropriate that the pump pulse width be smaller than both the Stark pulse width and the delay between the pulses in order to suppress adiabatic passage at the other crossing. In this adiabatic-diabatic scenario the system will follow the path shown in the *middle right frame* in Figure 3: The state vector will adiabatically follow the lower adiabatic state through the first crossing, whereas during the second crossing it will follow the diabatic state ψ_2 (rather than an adiabatic state) and remain there until the end of the interaction. The net result is complete population transfer from state ψ_1 to state ψ_2. It should be appreciated that the adiabatic and diabatic intervals can occur in either order: The pump pulse may either precede or follow the Stark pulse.

The SCRAP technique resembles the early experiment by Loy (16), who used adiabatic quasistatic pulses of about 5 ms duration to induce Stark shifts. However, he induced two sequential population transfers per pulse—excitation for the leading edge and deexcitation for the trailing edge of each pulse—resulting in no net population transfer. In contrast, the time delay between the pump and Stark pulses in SCRAP ensures that population transfer takes place at just one of the crossings, thus leading to overall population transfer.

It should be obvious from the above description that complete population transfer will only occur within finite ranges of values of the various interaction parameters. For example, in order that there be level crossings the static detuning Δ_0 must be smaller than the maximum Stark shift S_0 and must have the same sign as S_0. Also, the pump pulse should be strong enough to ensure adiabatic passage at one of the crossings, but weak enough to prevent adiabatic passage at the other. For Gaussian pulse shapes, $\Omega(t) = \Omega_0 \exp(-t^2/T_P^2)$ and $S(t) = S_0 \exp[-(t-\tau)^2/T_S^2]$, the latter requirements lead to the conditions (53)

$$1 \ll \frac{(\Omega_0 T_S)^2}{\Delta_0 \tau} \ll \exp\left(8\tau^2/T_P^2\right). \qquad 17.$$

These conditions set upper and lower limits on the peak pump Rabi frequency Ω_0 and the static detuning Δ_0.

The SCRAP technique benefits from the fact that strong fixed-frequency long-wavelength pulsed-laser radiation, suitable for Stark shifting the levels, is often available because it is used to generate (by frequency conversion) the visible or ultraviolet radiation needed for the pump interaction. Moreover, its pulse width is longer than the pump pulse width, which is beneficial for SCRAP.

As with simple adiabatic passage, the SCRAP technique can produce population transfer in an ensemble of atoms having a distribution of Doppler shifts. The peak value of the Stark shift sets the maximum detuning that can be accessed; in turn, this sets the range of Doppler shifts for which population transfer can be produced.

2.2.2 Experimental Demonstration
The first experimental demonstration of SCRAP was achieved in metastable helium (53). The initial state $1s2s\ ^3S_1$ was coupled to the target state $1s3s\ ^3S_1$ by a two-photon transition induced by an 855-nm pump laser pulse with a pulse duration of 3 ns (half width at $1/e$ of intensity), as shown in Figure 4 (*left*). The Stark shift was induced by a 1064-nm laser pulse with a pulse duration of 4.6 ns, delayed by 7 ns with respect to the pump pulse. Both laser pulses were mildly focused into the atomic beam. Nearly complete population transfer was observed with typical intensities of 20–30 MW/cm^2 for the pump pulse and 200–500 MW/cm^2 for the Stark pulse.

As an example, Figure 4 (*right*) displays the transfer efficiency plotted versus the static two-photon detuning $\Delta_0 = \omega_0 - 2\omega_P$. Nearly complete population transfer is observed within a certain detuning range, as predicted by analytical estimates. For large positive detuning, the adiabatic condition at the first crossing is violated, and the transfer efficiency decreases. For small positive detunings (near $\Delta_0 = 0$),
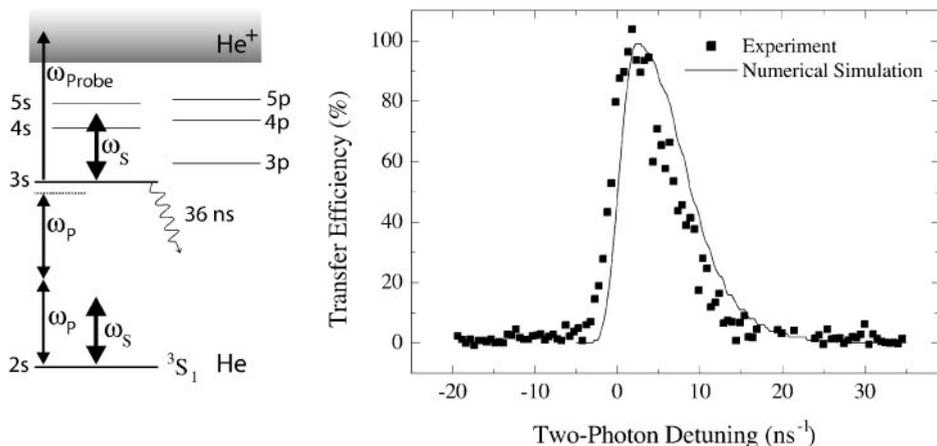
Figure 4 (*Left*) Simplified energy-level diagram of helium atom used in the demonstration of Stark-chirped rapid adiabatic passage. (*Right*) Population transfer efficiency versus the static two-photon detuning Δ_0.

the diabatic condition at the second crossing is violated, and the transfer efficiency decreases. For $\Delta_0 < 0$ and for very large positive Δ_0, there are no level crossings at all, and little population is transferred to the excited state.

An interesting extension of SCRAP—potentially very important for molecules—is the application of two sequential SCRAP processes. For example, the first SCRAP can transfer the population from the electronic ground state to an electronically excited state via a two-photon excitation. The second SCRAP then transfers the population to a target state in the electronic ground state, e.g. a highly vibrationally excited state. The second step can take place via a one-photon process [(2 + 1)-SCRAP] or by a two-photon process [(2 + 2)-SCRAP]. It is easily seen that only one Stark-shifting laser is needed in the (2 + 1)-SCRAP scheme. The (2 + 2)-SCRAP can be realized even without a separate Stark pulse because the Stokes pulse can serve as Stark pulse for the pump transition, and the pump pulse can induce the Stark shift for the Stokes transition (53).

2.3 Multiple Level Crossings

The concept of adiabatic passage via level crossing is not limited to two-state systems. Multi-state systems, however, have multiple eigen energies that often exhibit numerous avoided crossings. Such systems can be quite complicated in general, but there are a number of cases in which one can prescribe simple recipes for successful navigation to the desired target state (54–58).

2.3.1 Electronic Ladder Climbing Using a Single Pulse Adiabatic passage has been extended to a three-state ladder system by Noordam and co-workers in
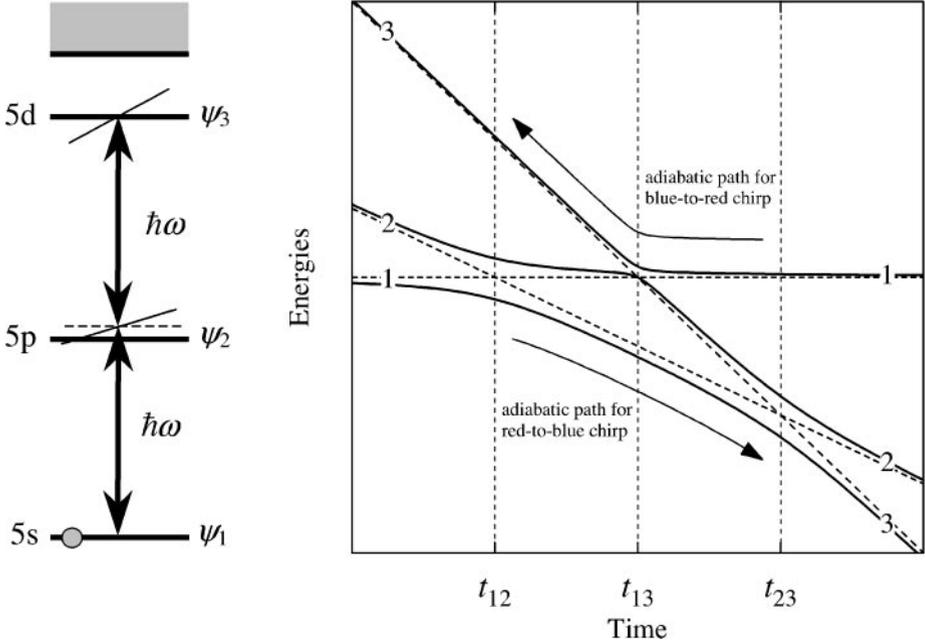
Figure 5 Linkage diagram (left) and energy diagram (right) in chirped-pulse climbing of the three-state electronic ladder 5s-5p-5d in rubidium atom. The dashed lines show the diabatic energies, and the blue solid curves show the adiabatic energies.

several experiments on the 5s-5p-5d transition in rubidium, shown in Figure 5 (40–44). Because the two single-photon transitions have very close Bohr frequencies (780.2 nm for 5s-5p and 775.9 nm for 5p-5d), it is possible to excite both transitions with the same femtosecond pulse. Virtually complete population transfer from the 5s state to the 5d state has been achieved both with red-to-blue and blue-to-red frequency chirp, as shown in Figure 6. However, the transfer mechanisms are different for the two chirps because, unlike the two-state case, multi-state systems are not generally invariant to the detuning signs.

The two transfer mechanisms are readily revealed by examining the adiabatic energies of the Hamiltonian describing the three-state ladder excitation,

$$
\mathsf{H}(t) = \hbar \begin{bmatrix} 0 & \frac{1}{2}\Omega_{12}(t) & 0 \\ \frac{1}{2}\Omega_{12}(t) & \Delta_2 & \frac{1}{2}\Omega_{23}(t) \\ 0 & \frac{1}{2}\Omega_{23}(t) & \Delta_3 \end{bmatrix}. \tag{18}
$$

The two detunings are given by differences between Bohr frequencies and multiple photon frequencies: $\hbar\Delta_2(t) = E_2 - E_1 - \hbar\omega(t), \hbar\Delta_3(t) = E_3 - E_1 - 2\hbar\omega(t)$, where we have denoted the 5s, 5p, and 5d states as ψ_1, ψ_2, and ψ_3, respectively. The two Rabi frequencies $\Omega_{12}(t)$ and $\Omega_{23}(t)$ (taken as real-valued without loss of
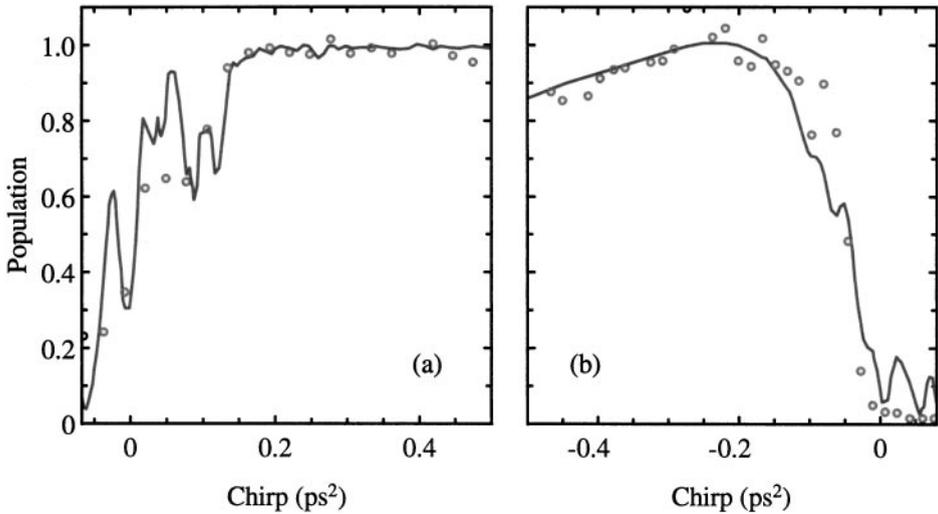
Figure 6   Population of the upper state 5*d* in the three-state ladder 5*s*-5*p*-5*d* in rubidium atom versus the pulse chirp. (*Left*) Red-to-blue chirp. (*Right*) Blue-to-red chirp. The dots are experimental data and the curves are numeric simulations. Adapted from (40) with permission.

generality) have the same time dependence (matching the laser pulse envelope), but generally different magnitudes owing to different transition dipole moments.

For red-to-blue chirp the transfer occurs via the adiabatic state with the lowest energy in Figure 5 because this state connects state ψ_1 initially with state ψ_3 at the end. While moving along this eigen energy the system encounters two level crossings: first between states ψ_1 and ψ_2 and then between ψ_2 and ψ_3. The red-to-blue chirp is the intuitively correct one because then the laser pulse comes to resonance first with the $\psi_1 \leftrightarrow \psi_2$ transition (which has the smaller transition frequency) and then with the $\psi_2 \leftrightarrow \psi_3$ transition. Consequently, the population flows gradually from state ψ_1 to state ψ_2 via a level crossing and then via another level crossing from state ψ_2 to state ψ_3. If the evolution is not sufficiently adiabatic, some population may leak at the first crossing t_{12} to the adjacent adiabatic state; some of this population will return to the initial adiabatic state at the second crossing t_{23}. This will lead to oscillations in the population of state ψ_3 because of interference caused by the two possible paths from ψ_1 to ψ_3.

For the counterintuitive blue-to-red chirp the laser pulse comes to resonance first with the transition between the initially unpopulated states ψ_2 and ψ_3 and then with the $\psi_1 \leftrightarrow \psi_2$ transition. In this case we can use again the energy plot from Figure 5 because inverting the chirp sign is equivalent to inverting the time direction. Now the evolution progresses from right to left, and the system follows the adiabatic state with the highest energy; this state connects state ψ_1 initially with state ψ_3 at

the end. During its evolution along this adiabatic curve the system encounters only one level crossing t_{13} between the energies of the bare states ψ_1 and ψ_3. Because this adiabatic energy is far from the bare energy of the intermediate state ψ_2, the latter will never get appreciable population. In this respect, the counterintuitive chirp excitation resembles stimulated Raman adiabatic passage (STIRAP), which is described below. Moreover, this is the only path linking ψ_1 to ψ_3, which means that there will be no oscillations in the population of ψ_3. Finally, Figure 5 shows that the avoided crossing at t_{13} is narrower than those at t_{12} and t_{23}. Hence, adiabaticity is more difficult to achieve with blue-to-red than with red-to-blue chirp. All these features have been observed experimentally (40–44).

2.3.2 Vibrational Ladder Climbing Using a Single Pulse   Selective excitation of molecular vibrational levels has important potential applications in laser-controlled molecular dissociation. Such excitation requires ultrashort pulses to avoid rotational relaxation that takes place on a picosecond scale. Because the transition frequencies between successive vibrational levels v within a given electronic state differ very little, it is possible to move population along this excitation ladder by using a single chirped laser pulse, provided the chirp is large enough to compensate for the anharmonicity. By using chirped infrared (5 mm) femtosecond laser pulses, Noordam and co-workers have achieved a significant vibrational excitation in the ground electronic state in NO (anharmonicity about 1.5%). First they tuned a broadband pulse from a free-electron laser to the transition frequency of the ladder and found populations in vibrational states up to $v = 5$ (48). Then they observed that the transfer was considerably enhanced when the laser frequency was blue-to-red chirped so as to follow the anharmonicity of the vibrational ladder (49). Compared with the thermal populations, the enhancement was 15 times for $v = 1$ and 700 times for $v = 3$. Furthermore, because there are many paths that lead to a certain rotational state of a high vibrational state, the total population in the ro-vibrational excited states oscillated as a function of the chirp (49). Finally, it has been suggested that vibrational excitation by a single chirped pulse can lead to efficient photodissociation (59–64).

2.3.3 Vibrational Ladder Climbing Using a Pair of Pulses: Raman Chirped Adiabatic Passage   Chelkowski & Gibson (65) and Chelkowski & Bandrauk (66) proposed the technique of Raman-chirped adiabatic passage (RCAP) as a tool for robust and efficient excitation of high vibrational levels in molecules. RCAP employs two laser pulses—pump and Stokes—both of which may be far off their respective single-photon resonances. Figure 7a illustrates the level linkage in RCAP. A successive step-by-step climbing of the vibrational ladder can eventually lead to vibrational dissociation of the molecule. In the original proposal (65), the pump laser was chirped and the Stokes was monochromatic, resulting in frequency sweeping of the two-photon resonance between the initial and final states in each Λ-subsystem in the chain; the feasibility of this scheme has been confirmed numerically.
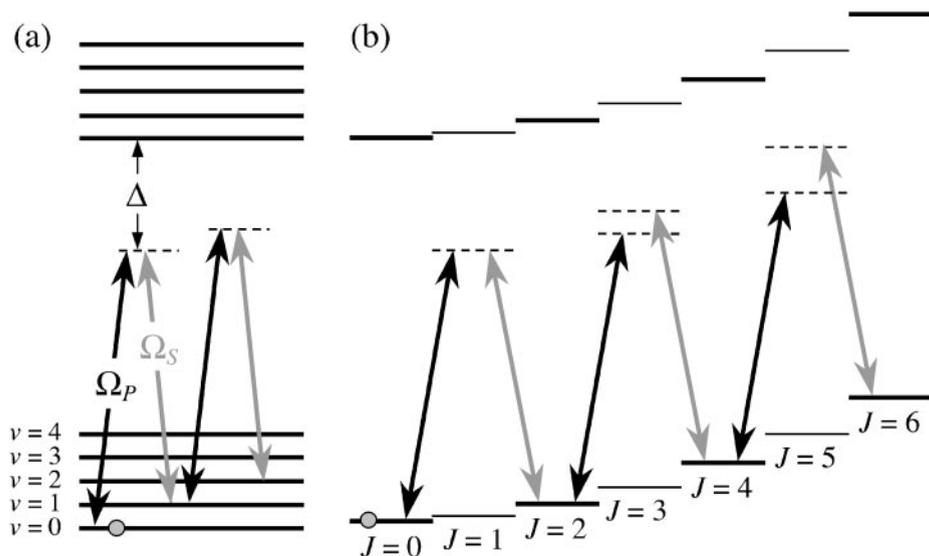
Figure 7 (*a*) Linkage diagram for vibrational-ladder climbing by a pair of chirped pulses (Raman-chirped adiabatic passage scheme). (*b*) Linkage diagram for rotational-ladder climbing by a pair of chirped pulses (molecular centrifuge).

Davis & Warren (67) have shown in calculations for oxygen and chlorine that a similar scheme with two chirped pulses provides some additional advantages.

RCAP requires that the frequency difference of the two pulses be tuned across the two-photon transition frequency in each Λ-subsystem, but it provides freedom in choosing each laser frequency, i.e. the location of the "virtual" states shown by dashed lines in Figure 7*a*. This avoids the necessity for ultraviolet lasers (often needed if coupling to the nearest electronic state is used) and allows the use of near infrared light, where short-pulse laser technology is well developed and can provide sufficient intensities to drive far off-resonance Raman couplings.

2.3.4 Rotational Ladder Climbing Using a Pair of Pulses Recently, Karczmarek et al (68) suggested that a ladder of rotational states can be efficiently excited using a pair of chirped infrared laser pulses with opposite circular polarizations and opposite chirps. Such pulses can induce consecutive level crossings in the chain of serial two-photon Raman transitions between neighboring rotational states with $J = 0, 2, 4, \ldots$, whose energies increase approximately as $J(J + 1)$, as shown in Figure 6*b*. Hence, if the two pulses are sufficiently intense to enable adiabatic evolution, a significant fraction of the population in the low-J states can be driven up the excitation ladder. This scheme for rotational excitation can be viewed as a variant of RCAP. When the rotation becomes sufficiently rapid, above

a certain threshold value of J, the molecular bond can no longer withstand the centrifugal force, and the molecule dissociates into two fragments (68).

Very recently, this scheme—called an optical centrifuge for molecules—has been successfully demonstrated experimentally (69) in Cl_2. Laser-induced dissociation has been achieved by inducing excitation up to states with $J = 420$, using chirped near-infrared laser pulses. In this experiment the rate of rotation was accelerated in 50 ps from 0 to 5 THz, at which rate the rotational energy approximately equals the bond energy. Thus, dissociation was achieved in a time scale shorter than the rotational relaxation time (70 ps), at a rate of about one Raman transition $J \rightarrow J + 2$ per 200 fs.

2.3.5 Chirped Excitation of a Manifold of Closely Spaced Levels
An interesting situation arises when a chirped laser pulse couples an initially populated state ψ_1 to a manifold of several levels $\psi_2, \psi_3, \ldots, \psi_N$ simultaneously. The energy diagram of such a coupled system, displayed in Figure 8a, shows that adiabatic evolution can produce a very selective excitation even if the Fourier bandwidth of the laser pulse is larger than the level spacing within the manifold. Indeed, for red-to-blue chirp the system will follow from left to right the lowest adiabatic energy, which links the initial state ψ_1 to the lowest unperturbed state ψ_2 of the manifold. In contrast, for blue-to-red chirp the system will follow from right to left the highest adiabatic energy, linking state ψ_1 to the highest unperturbed state ψ_N. Therefore,
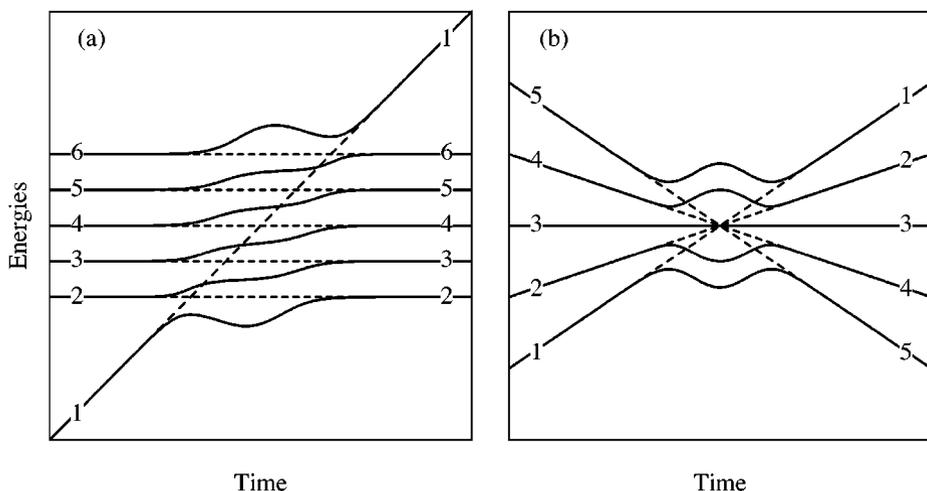
Figure 8   (*a*) Energy diagram for a system in which a ground state is simultaneously coupled by a chirped laser pulse to a manifold of five states. (*b*) Energy diagram in a five-state bowtie model. The dashed lines show the unperturbed (diabatic) energies, and the solid curves show the adiabatic energies.

the chirp sign alone determines if the population will be directed toward the lowest or the highest state of the manifold. Warren and co-workers (32) demonstrated this excitation scheme experimentally on the 3s-3p transition in sodium. Red-to-blue chirped picosecond pulses populated predominantly the lower fine-structure level $3p^2P_{1/2}$, whereas blue-to-red chirped pulses placed the population onto the upper fine-structure level $3p^2P_{3/2}$.

It is interesting to note that this linkage pattern allows an exact analytic solution (not just in the adiabatic limit, but also for any interaction parameters) in the case of constant chirp (i.e. linear detuning) and constant Rabi frequency over infinite time interval; this is the so-called Demkov-Osherov model (70, 71). Somewhat unexpectedly, the transition probabilities in this model are extremely simple and given by products of Landau-Zener probabilities for transition or no transition applied at the relevant crossings. For example, the transition probability from state ψ_1 to state ψ_4 with red-to-blue chirp (left-to-right direction in Figure 8a) is $p_{12}p_{23}(1 - p_{34})$, where p_{mn} is the Landau-Zener probability (16) for nonadiabatic transition at the crossing between states ψ_m and ψ_n.

2.3.6 The Bowtie Model   Another interesting example of adiabatic passage is the so-called bowtie model (72–77), whose energy diagram is displayed in Figure 7b. It occurs in a sequentially coupled evenly spaced *N*-state ladder, excited by the same laser pulse. In this case the RWA energy of the *n*th state is $E_n - E_1 - n\hbar\omega$. Adiabatic sweep of frequency through resonance will transfer all population from the lowest to the highest energy state, for either sign of the chirp. A bowtie-type linkage can also occur in an rf-pulse-controlled Bose-Einstein condensate output coupler (78, 79).

3.   ADIABATIC POPULATION TRANSFER USING SEQUENTIAL PULSES

The technique of stimulated Raman adiabatic passage (STIRAP) (56, 80–84) uses the coherence of two pulsed laser fields to achieve a complete population transfer from an initially populated state ψ_1 to a target state ψ_3 via an intermediate state ψ_2 (see Figure 1b). Instead of applying the pulses in the intuitive sequence, where the pump pulse precedes the Stokes pulse (as with SEP), the Stokes pulse precedes the pump pulse (counterintuitive ordering). If there is sufficient overlap of the two pulses and if the pulses are sufficiently strong that the time evolution is adiabatic, then complete population transfer occurs between states ψ_1 and ψ_3.

3.1   Stimulated Raman Adiabatic Passage in Three-State Systems: Theory

3.1.1 Background   At first glance, the pulse sequence of STIRAP seems strange (counterintuitive): The first pulse to act on the system (the Stokes pulse) connects

two initially unpopulated states. The STIRAP mechanism can be understood when we examine the eigenvalues and the eigen states of the Hamiltonian driving the probability amplitudes $\mathbf{C}(t) = [C_1(t), C_2(t), C_3(t)]^T$ of the Λ-system,

$$H(t) = \hbar \begin{bmatrix} 0 & \frac{1}{2}\Omega_P(t) & 0 \\ \frac{1}{2}\Omega_P(t) & \Delta_P & \frac{1}{2}\Omega_S(t) \\ 0 & \frac{1}{2}\Omega_S(t) & \Delta_P - \Delta_S \end{bmatrix}. \qquad 19.$$

Here $\Omega_P(t)$ and $\Omega_S(t)$ are the Rabi frequencies of the pump and Stokes pulses, respectively, and Δ_P and Δ_S are the single-photon detunings of the pump and Stokes lasers from their respective transitions, $\hbar\Delta_P = E_2 - E_1 - \hbar\omega_P$, $\hbar\Delta_S = E_2 - E_3 - \hbar\omega_S$. An essential condition for STIRAP is the two-photon resonance between states ψ_1 and ψ_3, $\Delta_P = \Delta_S = \Delta$. Then the three instantaneous eigenstates of $H(t)$ (the adiabatic states) are given by

$$\Phi_+(t) = \psi_1 \sin\vartheta(t)\sin\varphi(t) + \psi_2 \cos\varphi(t) + \psi_3 \cos\vartheta(t)\sin\varphi(t), \qquad 20.$$

$$\Phi_0(t) = \psi_1 \cos\vartheta(t) - \psi_3 \sin\vartheta(t), \qquad 21.$$

$$\Phi_-(t) = \psi_1 \sin\vartheta(t)\cos\varphi(t) - \psi_2 \sin\varphi(t) + \psi_3 \cos\vartheta(t)\cos\varphi(t), \qquad 22.$$

where the mixing angles $\vartheta(t)$ and $\varphi(t)$ are defined (modulo π) as $\vartheta(t) = \arctan[\Omega_P(t)/\Omega_S(t)]$, $\varphi(t) = \frac{1}{2}\arctan[\sqrt{\Omega_P^2(t) + \Omega_S^2(t)}/\Delta]$. These eigen states have the following eigen frequencies:

$$\varepsilon_0(t) = 0, \quad \varepsilon_\pm(t) = \frac{1}{2}\Delta \pm \frac{1}{2}\sqrt{\Delta^2 + \Omega_P^2(t) + \Omega_S^2(t)}. \qquad 23.$$

STIRAP is based on the zero-eigenvalue adiabatic state $\Phi_0(t)$, which is a coherent superposition of the initial state ψ_1 and the final state ψ_3 only. This adiabatic state has no component of the excited state ψ_2, and hence it has no possibility of radiatively decaying; it is a trapped state (of population) or a radiatively dark state (85–89). For the counterintuitive pulse ordering the relations $\Omega_P(t)/\Omega_S(t) \overset{t\to-\infty}{\longrightarrow} 0$ and $\Omega_P(t)/\Omega_S(t) \overset{t\to+\infty}{\longrightarrow} \infty$ apply; hence, as time progresses from $-\infty$ to $+\infty$, the mixing angle $\vartheta(t)$ rises from 0 to $\pi/2$. Consequently, the adiabatic state $\Phi_0(t)$ evolves from the bare state ψ_1 to a superposition of states ψ_1 and ψ_2 at intermediate times and finally to the target state ψ_3 at the end of the interaction; thus, state $\Phi_0(t)$ links adiabatically the initial state ψ_1 to the target state ψ_3. Because the Hamiltonian is explicitly time dependent, diabatic transitions between the adiabatic states will occur. The goal is to reduce the diabatic transition rates to negligibly small values. When the system can be forced to stay in the dark state at all times, a complete population transfer from ψ_1 to ψ_3 will be achieved, as shown in Figure 9. This can be realized by ensuring adiabatic evolution; then no transitions between the adiabatic states can take place. The adiabatic condition requires
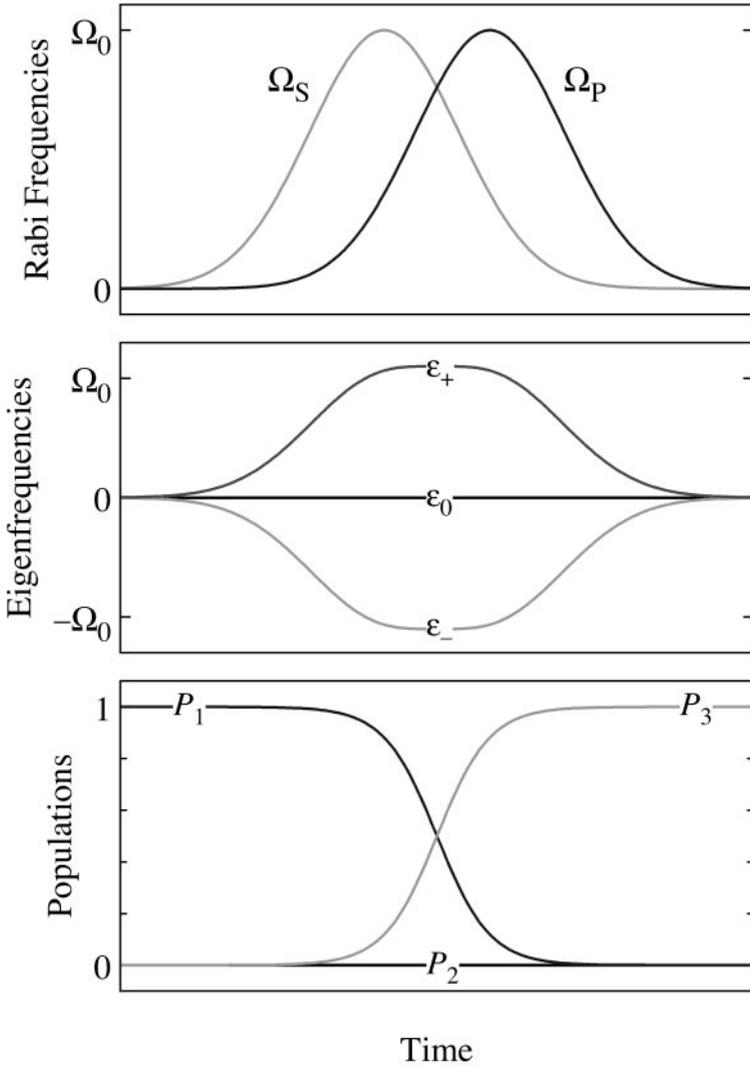
Figure 9 Time dependences of the pump and Stokes Rabi frequencies (*top*), the eigen frequencies (*middle*), and the populations (*bottom*) in three-state stimulated Raman adiabatic passage.

that the coupling between each pair of adiabatic states is negligible compared with the difference between the energies of these states. With respect to the dark state $\Phi_0(t)$, the adiabatic condition reads (5, 6)

$$\left|\varepsilon_0 - \varepsilon_\pm\right| \gg \left|\langle\dot\Phi_0|\Phi_\pm\rangle\right|. \qquad 24.$$

On one-photon resonance ($\Delta = 0$) the adiabaticity condition simplifies and becomes (81)

$$\sqrt{\Omega_P^2 + \Omega_S^2} \gg \left|\dot{\vartheta}\right| \propto T^{-1}, \qquad 25.$$

where T is the pulse width. Assuming that the pump and Stokes pulses have the same peak Rabi frequency Ω_0, this condition can be written as $\Omega_0 T \gg 1$. Hence, adiabaticity demands a large pulse area. In practical applications the pulse area should exceed 10 to provide efficient population transfer. In terms of incoherent excitation, the large pulse area means saturation of the transitions.

Once the conditions for STIRAP are fulfilled (two-photon resonance between states ψ_1 and ψ_3, counterintuitive pulse ordering, and adiabatic evolution), a complete population transfer from ψ_1 to ψ_3 is guaranteed. Moreover, because the dark state does not involve the intermediate state ψ_2, the latter remains unpopulated during the transfer, which means that its properties, such as radiative decay, have little impact on the transfer efficiency. This is a remarkable feature of STIRAP, which allows efficient population transfer on time scales exceeding the intermediate-state lifetimes. For example, such a situation arises in the implementation of STIRAP with continuous lasers when the atomic beam crosses two spatially displaced and partially overlapping continuous-wave (cw) laser beams at right angles (81, 90). The time it takes for the atoms or molecules to cross the laser beams is about two orders of magnitude longer than the lifetime of the excited state, thus prohibiting any population transfer by intermediate storage in the excited state, e.g. by stimulated emission pumping. By contrast, STIRAP still maintains a transfer efficiency of 100%, because the upper state is never populated.

3.1.2 Intuitive versus Counterintuitive Pulse Order   When both the pump and Stokes lasers are on resonance with their respective transitions, the two opposite pulse sequences lead to qualitatively different results: The intuitive sequence produces generalized Rabi oscillations, while the counterintuitive sequence induces complete population transfer to state ψ_3 (91–94). When the two lasers are tuned off the respective single-photon resonances, while maintaining the two-photon resonance, both pulse sequences can lead to complete population transfer from state ψ_1 to state ψ_3 (92, 94). This result is easily explained when the single-photon detuning Δ is large; then the intermediate state ψ_2 can be eliminated adiabatically (92, 94). The resulting effective two-state problem involves a coupling $\Omega_{\text{eff}} = \Omega_P \Omega_S / 2\Delta$ and a detuning $\Delta_{\text{eff}} = (\Omega_P^2 - \Omega_S^2)/2\Delta$. Obviously, for delayed pulses the detuning Δ_{eff} passes through resonance at the time t_0 when $\Omega_P(t_0) = \Omega_S(t_0)$; this level crossing leads, in the adiabatic limit, to complete population transfer for both pulse orders because the order reversal is equivalent to the unimportant change of sign in Δ_{eff}. However, there is still a significant difference between the two pulse sequences: The intermediate state ψ_2 receives some transient population for the intuitive sequence, whereas it remains unpopulated for the counterintuitive sequence. Hence, if the lifetime of state ψ_2 is comparable to or shorter than the

excitation duration, then efficient population transfer can be achieved only with the counterintuitive pulse sequence.

3.1.3 Dependence on the Interaction Parameters Various aspects of STIRAP have been studied in detail. Among these are the effects of nonadiabatic transitions (95–101) and in particular, the manner in which the adiabatic limit is approached (95–98). Furthermore, analytical expressions for the single-photon linewidth (102) and the two-photon linewidth (103, 104, 105) have been derived. The results have demonstrated that STIRAP is much less sensitive to single-photon detuning (because the single-photon linewidth grows with the square of the pulse area) than to two-photon detuning (in which the linewidth increases only approximately linearly with the pulse area); Figure 10 shows an example. The influence of spontaneous
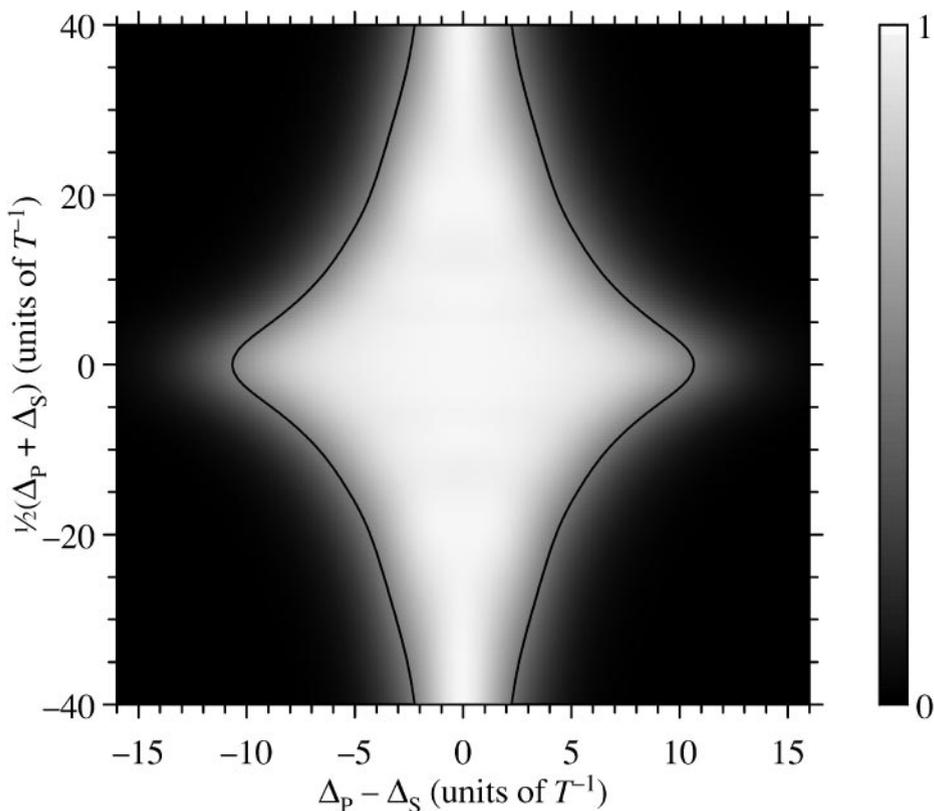
Figure 10 Numerically calculated transfer efficiency in stimulated Raman adiabatic passage plotted versus the sum and the difference of the pump and Stokes detunings (i.e. versus the single-photon and two-photon detunings) for Gaussian pulse shapes, $\Omega_P = \Omega_0 \exp[-(t-\tau)^2/T^2]$, $\Omega_S = \Omega_0 \exp[-(t+\tau)^2/T^2]$, with $\Omega_0 T = 20$, $\tau = 0.5T$. The curves show the $P_3 = 0.5$ value.

emission from the intermediate state ψ_2 has also been studied, including decay both within the Λ-system (back to states ψ_1 and ψ_3) (106) and to other states (107, 108). Finally, the effects of multiple intermediate states (109, 110) and multiple final states (111, 112) have been explored, as has STIRAP beyond the RWA approximation (113).

3.2 STIRAP in Three-State Systems: Experiment

3.2.1 Experimental Demonstration with cw Lasers   After preliminary, yet incomplete, results (114), Bergmann et al achieved the first convincing experimental demonstration of STIRAP in Na$_2$ (81). A beam of sodium dimers crossed two spatially displaced but partially overlapping cw laser beams. When the sodium dimers interacted first with the Stokes laser (counterintuitive pulse ordering) complete population transfer was observed from the initial level ($v = 0$, $J = 5$) to the final level ($v = 5$, $J = 5$) of the Na$_2$ molecules in their electronic ground state $X^1\Sigma_g^+$ via an intermediate level ($v = 7$, $J = 6$) of the excited electronic state $A^1\Sigma_u^-$. The duration of the interaction with combined pulses (the time required for a molecule to traverse the two laser beams) was about 0.2 μs. Because the interaction time was much longer than the excited-state lifetime and because the sodium dimers have relatively strong transition moments, only moderate laser intensities were needed to induce large pulse areas. Typical intensities in the range of 100 W/cm^2, provided by cw lasers mildly focused to a few hundred μm into the molecular beam, were sufficient to observe adiabatic passage.

STIRAP has also been observed in metastable neon in a similar crossed-beam geometry (90, 115, 116). In the Theuer & Bergmann experiment (90) the population was transferred from state $2p^53s\,^3P_0$ to state $2p^53s\,^3P_2$ via the intermediate state $2p^53p\,^3P_1$. The intensities used in the experiment, typically a few W/cm^2, were again provided by cw radiation, focused into the atomic beam by cylindrical lenses. Although the typical time required for passage of atoms across the laser beams was more than 20 times longer than the radiative lifetime of the excited intermediate state, no more than 0.5% of the population was detected in this state.

Figure 11 displays a characteristic signature for STIRAP. In this figure the transfer efficiency is plotted versus the spatial displacement between the pump and Stokes laser beams, i.e. versus the pulse delay from the viewpoint of the Ne* atoms. Positive displacement (*left*) corresponds to counterintuitive pulse order (Stokes before pump) and negative displacement (*right*) to intuitive order (pump before Stokes). The population in the target state was detected by a probe laser via laser-induced fluorescence. When the Stokes beam was shifted too far upstream (far left in the figure), it was excluded from the interaction because there was no overlap with the pump pulse; in this case about 25% of the population was optically pumped into the target state because the pump laser excited the atoms to the intermediate state from which they decayed radiatively. As the Stokes beam was shifted toward the pump beam, while still preceding it, the transfer efficiency
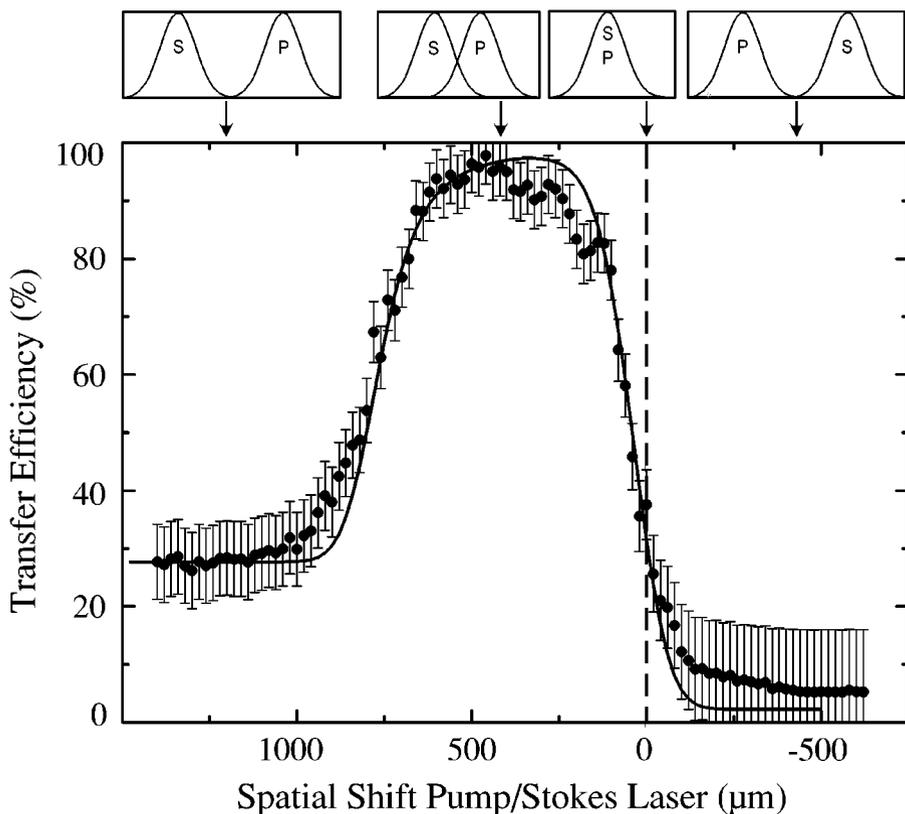
Figure 11 Transfer efficiency versus displacement between pump and Stokes pulses in Ne* experiment. The broad plateau, showing nearly complete population transfer for counterintuitive pulse sequence, is a typical stimulated Raman adiabatic passage signature, as contrasted with the low efficiency for intuitively ordered pulses. The dots are experimental data and the curve shows numeric simulation.

increased dramatically and reached almost unity. When the axes of the two lasers coincided, the transfer efficiency dropped to about 25%. Virtually no transfer was observed when the Stokes beam was moved farther downstream so that the Ne* atoms encountered the pump laser first (intuitive pulse ordering). In this configuration the atoms were initially in a bright adiabatic state and population was transferred to the intermediate state, from which it decayed via a two-step cascade to the ground state of Ne (i.e. out of the laser-coupled three-state system) by spontaneous emission of vacuum ultraviolet radiation. The broad plateau for counterintuitive laser order is a characteristic feature of STIRAP, and it indicates the robustness of the population transfer.
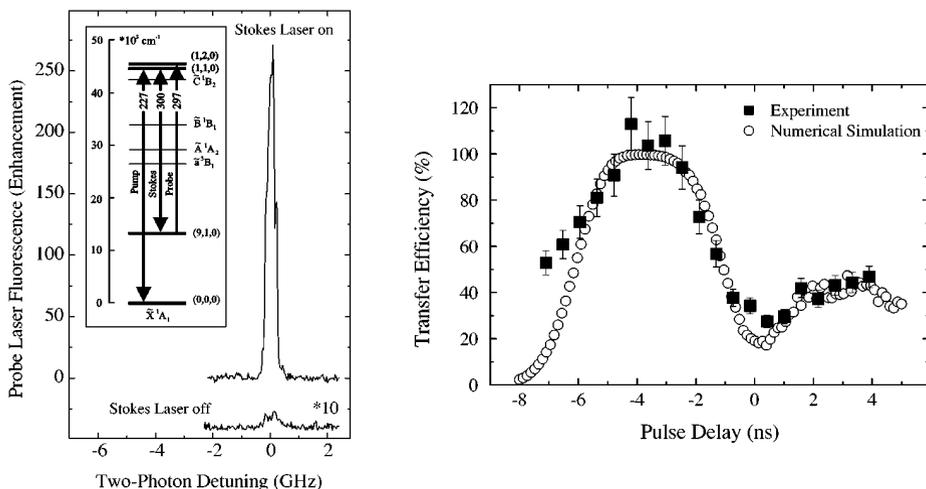
3.2.2 Experimental Demonstration with Pulsed Lasers   A very interesting and important application of STIRAP is the selective excitation of high-lying vibrational levels in molecules. In most molecules the first electronically excited states have energies more than 4 eV above the ground state. Therefore, a Raman-type linkage from the vibrational ground level to a high vibrational level requires ultraviolet lasers. Strong ultraviolet radiation is most readily provided by frequency conversion techniques involving high-intensity pulsed lasers. Furthermore, because the molecular transition dipole moments are usually considerably smaller than for atoms, the adiabaticity condition is difficult to satisfy with cw lasers. Sufficiently strong light intensity, and hence large enough couplings, can be delivered only by pulsed lasers. Pulsed lasers, however, often have inferior coherence properties, e.g. they suffer from phase fluctuations and frequency chirping. A careful analysis of the effect of imperfect laser coherence on the STIRAP efficiency provides the modified adiabaticity condition, $\Omega_0 T \gg [1 + (\Delta\omega/\Delta\omega_{TL})^2]^{1/2}$ (117), where $\Delta\omega_{TL}$ is the transform-limited bandwidth of the pulse and $\Delta\omega$ is its actual bandwidth. The adverse effect of imperfect laser coherence derives from the fact that both phase fluctuations and frequency chirp correspond to time-dependent changes in the laser frequencies. Unless these changes are correlated (e.g. if the pump and Stokes pulses are derived from the same laser), they will result in time-dependent detuning from two-photon resonance. The two-photon detuning induces nonadiabatic couplings between the dark state and the other adiabatic states that reduce the transfer efficiency. These population losses can be reduced by increasing the laser intensity, thereby suppressing nonadiabatic transitions. For conventional nanosecond lasers that are not specially designed to yield nearly transform-limited pulses, the ratio $\Delta\omega/\Delta\omega_{TL}$ is typically bigger than 10. According to the above estimate, the intensity needed for STIRAP has to be increased by a factor of 100 with respect to transform-limited pulses. Although in principle it is possible to obtain higher intensities by focusing the laser beam, this would be detrimental for most applications, in which large volumes of the molecular jet must be excited, e.g. in reactive scattering experiments. Therefore, it is almost impossible to satisfy the adiabaticity criterion for laser pulses whose bandwidth clearly exceeds the bandwidth of transform-limited pulses.

It is also useful to point out that if a pulse energy of 1 mJ were sufficient to ensure adiabatic evolution for a 1-ns laser pulse then the same degree of adiabaticity would require energy of 1 J for a 1-ps laser pulse. Indeed, this conclusion follows readily from the adiabatic condition when it is written as $\Omega_0^2 T \gg 1/T$ (for transform-limited pulses); obviously, the required pulse energy (which is proportional to $\Omega_0^2 T$) grows rapidly when the pulse duration T decreases. Still, this does not mean that long-pulse or cw lasers offer the best possibilities to implement STIRAP. Indeed, the product $\Omega_0 T$, which is proportional to the square root of the pulse energy times the pulse duration T, is typically largest for tunable laser sources of intermediate pulse duration, i.e. nanosecond lasers. Conventional tunable picosecond and femtosecond lasers typically cannot compensate for the

shorter pulse duration by an adequate increase in pulse energy. On the other hand, cw lasers may provide longer interaction times, but suffer from weak intensities.

STIRAP has been successfully demonstrated with nanosecond pulses in NO (118, 119) and SO_2 (120) molecules and in rubidium atoms (121). In NO, highly efficient and selective population transfer has been achieved in the electronic ground state from the $X^2\Pi_{1/2}(v = 0, J = \frac{1}{2})$ rovibrational state to the $X^2\Pi_{1/2}(v = 6, J = \frac{1}{2})$ state via the intermediate state $A^2\Sigma(v = 0, J = \frac{1}{2})$. The NO molecule provides an example of complications that may arise owing to hyperfine structure. What seems to be a 3-level system is actually a system of 18 sublevels. Because $^{14}N^{16}O$ has a nuclear spin of $I = 1$, each of the three levels is split into a pair of sublevels with $F = \frac{1}{2}$ and $F = \frac{3}{2}$, which in turn possess magnetic sublevels. For linearly polarized light, and when the pump and Stokes polarizations are parallel, the 18-state system decomposes into 2 independent 3-state systems (one with $F = \frac{3}{2}, m_F = \frac{3}{2}$ and another with $F = \frac{3}{2}, m_F = -\frac{3}{2}$) and 2 6-state systems for $m_F = \frac{1}{2}$ and $m_F = -\frac{1}{2}$. Because the hyperfine splitting of the initial level and the final level is large enough to be resolved experimentally, the complexity of the system can be further reduced. Thus, despite the complications, a nearly complete transfer has been achieved (118, 119).

The population transfer achieved in SO_2 molecules (120) is an example of STIRAP for a polyatomic molecule. The enormously increased density of levels, as compared with atoms or diatomic molecules, results in much smaller transition dipole moments. Nevertheless, efficient population transfer becomes possible with adequate laser power, when the level density in the final state is not too high. Figure 12 shows an example of population transfer from the rotational state 3_{03} of


Figure 12 Experimental demonstration of stimulated Raman adiabatic passage in SO_2 molecules versus two-photon detuning (*left*) and pulse delay (*right*). The inset in the left plot shows the level linkage.

the vibrational ground state (0, 0, 0) to the same rotational level of the (9, 1, 0) overtone in the electronic ground state $X\,^1A_1$ via the vibrational level (1, 1, 0) of the excited electronic state $C\,^1B_2$. The wavelengths were 227 nm for the pump and 300 nm for the Stokes laser (120). Pulse durations were 2.7 ns (half width at $1/e$ of maximum electric field) for the pump and 3.1 ns for the Stokes laser pulse. Typical laser intensities were 10 MW/cm^2, yielding Rabi frequencies of about 10^{10} s^{-1}. The population in the target state was probed by laser-induced fluorescence. The lower trace in Figure 12 (*left*) displays signal of the probe-laser-induced fluorescence from the final state (magnified 10 times) in the case in which only the pump pulse was present; then the final state was populated by spontaneous emission from the intermediate state. When the Stokes pulse was turned on and applied before the pump pulse (with an appropriate overlap between them) the final-state population increased by more than two orders of magnitude. When the delay between the pump and Stokes pulses was varied, the typical plateau region of complete population transfer for negative pulse delay was observed (Figure 12 *right*). For positive pulse delay, i.e. the case of SEP with the pump preceding the Stokes pulse, a transfer efficiency of about 25% was observed, as one expects from rate equation calculations.

3.2.3 STIRAP with Degenerate Levels   A problem that often arises when implementing STIRAP in real atoms and molecules is the existence of multiple intermediate and final states. These may be present owing to fine and/or hyperfine structure, Zeeman sublevels, or closely spaced rovibrational levels in polyatomic molecules. A detailed numerical, analytical, and experimental investigation of this problem has been presented in a series of papers on STIRAP in metastable neon atoms (122–124). It has been concluded that the presence of closely spaced levels near the intermediate and final state may pose a problem and even be detrimental for STIRAP. In particular, STIRAP can selectively populate a particular target level only if the two-photon linewidth is smaller than the level separation near this level.

A multi-state system has multiple eigen energies that may present a very complicated picture. For instance, narrow avoided crossings between the eigen energies may appear; if such avoided crossings involve the eigen state that provides the adiabatic linkage for STIRAP then the adiabatic path will be blocked and STIRAP may fail. The level scheme in the neon experiment (124) involves states with $J = 0$, 1, and 2, which means that there are $1 + 3 + 5 = 9$ magnetic sublevels in total. Figure 13 (*left*) shows these nine states, with several possible linkage patterns (determined by the dipole selection rules) for different polarizations of the pump and Stokes lasers. Figure 13 (*right*) shows the behavior of the final-state population as a function of the magnetic field, which lifts the Zeeman degeneracy, when the Stokes-laser polarization was parallel to the magnetic field and the pump polarization was perpendicular (124); the ensuing linkage pattern is shown in Figure 13c. The Stokes frequency was tuned to resonance with the Bohr frequency of the degenerate $(B = 0)$ $^3P_2 \leftrightarrow {}^3P_1$ transition, whereas the pump laser frequency was scanned across the resonance. For small magnetic field a single peak in the
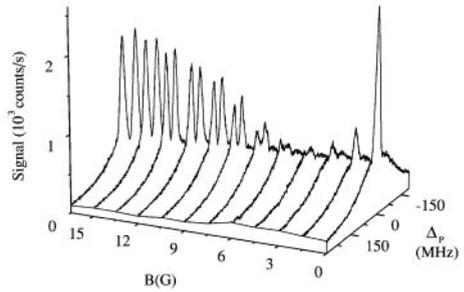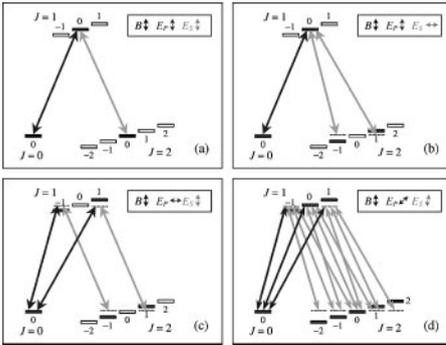
Figure 13   (*Left*) Linkage patterns in Ne* for various choices of pump and Stokes polarizations with respect to the direction of the magnetic field *B*. (*Right*) Population transfer in Ne* versus magnetic field strength.

target-state population was observed near resonance ($\Delta_P = 0$), because the $M = +1$ and $M = -1$ sublevels were too close to be resolved. For large magnetic field, the Zeeman splitting increased and a symmetric two-peaked structure emerged, indicative of populations of the $M = +1$ and $M = -1$ sublevels. A significant drop in the transfer efficiency was observed at intermediate magnetic field strengths. This drop was identified (124) as due to lack of adiabatic connectivity between the initial and final states, i.e. the adiabatic path between them was blocked because of interference from neighboring adiabatic states.

3.3   Extensions of STIRAP

3.3.1 Multi-State Chains   The success of STIRAP in three-state systems has encouraged its extension to multi-state chainwise-connected systems $\psi_1 \leftrightarrow \psi_2 \leftrightarrow \psi_3 \leftrightarrow \cdots \leftrightarrow \psi_N$ (90, 125–136). It has been discovered that multi-state systems behave differently when they involve odd and even numbers of states.

It has been found that for an odd number of states ($N = 2n + 1$) a STIRAP-like population transfer can take place for delayed and counterintuitively ordered pulses when all lasers are on resonance with the corresponding transitions or when only the even states in the chain are detuned from resonance (125–127). The transfer is carried out via a multi-level dark state that is a time-dependent coherent superposition of the odd states in the chain $\psi_1, \psi_3, \ldots, \psi_{2n+1}$. For example, the dark state in a five-state chain reads (125–127, 137, 138)

$$\Phi_0(t) = \frac{1}{v(t)} \left[\Omega_{23}(t)\Omega_{45}(t)\psi_1 - \Omega_{12}(t)\Omega_{45}(t)\psi_3 + \Omega_{12}(t)\Omega_{34}(t)\psi_5 \right], \quad 26.$$

where $v(t)$ is a normalization factor. It is easily seen that when the pulse $\Omega_{45}(t)$, driving the last transition, precedes the pulse $\Omega_{12}(t)$, driving the first transition, this state provides adiabatic connection between the initial state ψ_1 and the last state ψ_5 of the chain.

A particularly suitable system for multi-state STIRAP is the chainwise transition formed by the magnetic sublevels of a degenerate two-state system with $J_e = J_g$ or $J_g - 1$, driven by two delayed pulses with opposite circular polarizations. For example, if the system is prepared initially in the $M_g = -J_g$ ground-state sublevel (e.g. by optical pumping), then a STIRAP-like transfer to the $M_g = J_g$ sublevel can be achieved by applying a pulse of σ^- polarization (the Stokes) before a pulse of σ^+ polarization (the pump), i.e. in the counterintuitive order. As in STIRAP, the sublevels of the excited state remain unpopulated throughout the transfer if the interaction is adiabatic; however, the odd states in the chain—the sublevels of the ground state—do acquire some transient populations. In this particular system these transient intermediate-state populations are not a problem because these sublevels do not decay and there are no population losses. Indeed, multi-state STIRAP in such chainwise systems has been demonstrated experimentally by several groups (90, 129–132).

In more general multi-state chains, in which the transiently populated intermediate states can decay radiatively during the transfer, it is desirable to reduce their populations. It has been suggested (133) that these transient populations can be suppressed when the pulses coupling the intermediate transitions are much stronger than the pulses driving the first (the pump) and the last (the Stokes) transitions. A pulse sequence—straddle-STIRAP—has been proposed, in which all intermediate pulses arrive simultaneously with the Stokes pulse and vanish with the pump pulse.

The systems with an even number of states ($N = 2n$) behave very differently in the resonant case because they do not possess a dark state. Consequently, even when such a system is driven adiabatically by counterintuitively ordered resonant pulses, a STIRAP-like population transfer between the initial and final states of the chain cannot occur. Instead, the final-state population exhibits Rabi-like oscillations as the pulse intensities increase (128, 134, 139). These oscillations occur because at early times the initial state is equal to a superposition of adiabatic states (rather than to a single adiabatic state as in STIRAP), and so is the final state at late times; hence, there is interference between the different paths from the initial state to the final state.

When the intermediate states are off resonance while the initial state and final state are still on ($N - 1$)-photon resonance, chains with odd and even numbers of states behave quite similarly. In both cases a STIRAP-like transfer may or may not be possible, depending on the laser parameters, particularly on the intermediate detunings (134). For example, in a four-state system, STIRAP-like transfer may take place when the cumulative detunings of the two intermediate states have the same sign, $\Delta_2 \Delta_3 > 0$, whereas it is impossible if $\Delta_2 \Delta_3 \leq 0$. The reason is that in the former case an adiabatic state exists that links the initial and final states, whereas in the latter case, such an adiabatic connection is absent.

A dressed-state approach (135) provides a particularly clear picture of multi-state STIRAP, valid for both odd and even numbers of states. It is most useful when the pulse (or pulses) driving the intermediate transitions arrives before and vanishes
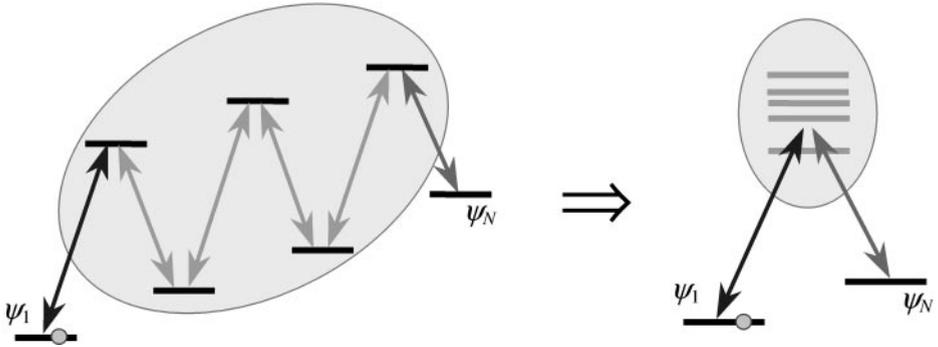
Figure 14   Linkage pattern for chain–stimulated Raman adiabatic passage (serial multi-Λ system) and equivalent parallel multi-Λ system, obtained by diagonalization of the subsystem comprising the intermediate states in the original chainwise system.

after the pulses driving the first (the pump) and the last (the Stokes) transitions, as in (133). Then the $N - 2$ intermediate states are coupled into a dressed subsystem (as shown in Figure 14), prior to the arrival of the pump and Stokes pulses. By changing the parameters of the dressing (control) pulse Ω_C (intensity and frequency), one can manipulate the properties of this dressed subsystem and thus, control the population transfer. By tuning the pump and Stokes lasers to one of the dressed eigen states Φ_k, the multi-state dynamics is essentially reduced to a system of three strongly coupled states: $\psi_1 \leftrightarrow \Phi_k \leftrightarrow \psi_N$; this paves the road for an efficient STIRAP-like population transfer from state ψ_1 to state ψ_N. Furthermore, it is beneficial if the dressing pulse(s) is constant (at least when the pump and Stokes pulses are present), because then the couplings between the dressed states vanish. Also, if the dressing pulse(s) is strong the spacing between the dressed energies is large. This makes the multi-Λ system resemble the single-Λ system in STIRAP and therefore place little population in the intermediate states.

The dressed picture also displays the difference between odd and even numbers of states in the on-resonance case (all detunings in the original chain equal to zero). For odd N, one of the dressed states is always on-resonance with the pump and Stokes lasers. In contrast, for even N, the pump and Stokes lasers are tuned in the middle between two adjacent dressed states, and the ensuing interference between different adiabatic paths leads to Rabi-like oscillations. Figure 15 shows the final-state population in a four-state system against the cumulative detunings from the two intermediate states ψ_2 and ψ_3. High transfer efficiency (the white zones) is achieved for sufficiently adiabatic evolution only if $\Delta_2 \Delta_3 > 0$, as discussed above. Near the dressed-state resonances (shown by parabolas) the transfer efficiency is high even when the evolution is not very adiabatic elsewhere (left frame). As the pulse areas increase (*right frame*), the two regions where $\Delta_2 \Delta_3 > 0$ (first and third quadrants) get filled with white (unity transfer efficiency), whereas no high transfer is possible in the $\Delta_2 \Delta_3 < 0$ regions (second and fourth quadrants).
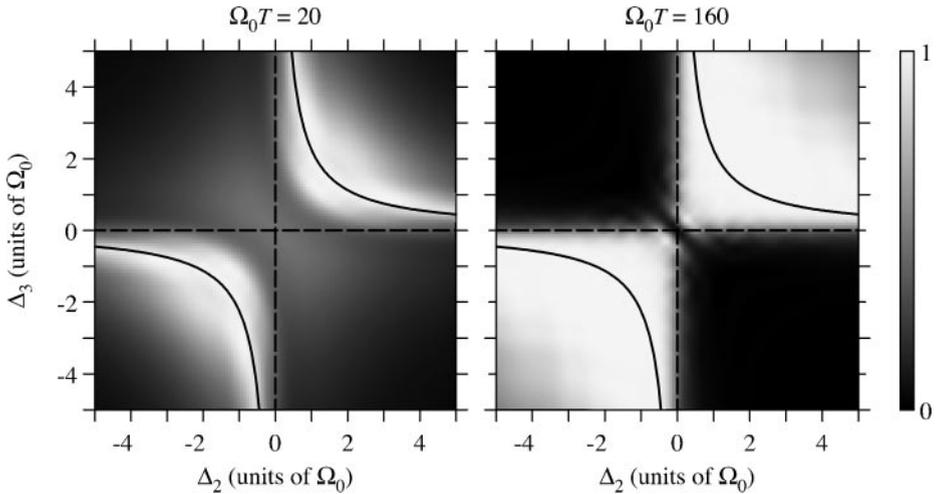
Figure 15   Numerically calculated transfer efficiency for chain-stimulated Raman passage in a four-state system versus the two intermediate-state detunings for $\Omega_P = \Omega_0 \exp[-(t - \tau)^2/T^2]$, $\Omega_S = \Omega_0 \exp[-(t + \tau)^2/T^2]$, $\Omega_C = 3\Omega_0$, with $\tau = 0.5T$ and $\Omega_0 T = 20$ (*left*) and $\Omega_0 T = 160$ (*right*). The curves show the two dressed-state resonances.

3.3.2 Population Transfer via Continuum   A few years ago it was suggested (140, 141) that a continuum can serve as an intermediary for population transfer between two discrete states in an atom or a molecule by using a sequence of two counterintuitively ordered delayed laser pulses. This intriguing scheme—which has yet to be demonstrated experimentally—can be seen as a variant of STIRAP in which the discrete intermediate state is replaced by a continuum of states. The advantage of this scheme with respect to STIRAP would be that only one tunable laser is needed, because a continuum offers a continuous range of possible combinations to match the pump and Stokes laser frequencies to the two-photon resonance between the initial and target states. The Carroll-Hioe analytic model (140, 141), which involves an infinite quasi-continuum of equidistant discrete states, equally strongly coupled to the two bound states, suggests that complete population transfer is possible, the ionization being suppressed. The physical reason for this unexpected conclusion (because a continuum is traditionally seen as an incoherent medium) is closely related to the laser-induced continuum structure (142–145) created in the structureless, flat continuum by the Stokes laser. Another finding supporting this scheme is that, as in a discrete three-state Λ-system, there exists a dark state—a coherent superposition of the two bound states that is immune to ionization.

Nakajima et al (146) later demonstrated, however, that the completeness of the population transfer in the Carroll-Hioe model derives from the very stringent restrictions of the model that are unlikely to be met in a realistic physical system with a real continuum, in particular with a nonzero Fano parameter and Stark shifts (147).

It has subsequently been recognized that although complete population transfer is unrealistic, significant partial transfer may still be feasible (148–153). It has been shown that, at least in principle, the detrimental effect of the nonzero Fano parameter and the Stark shifts can be compensated by using the Stark shifts induced by a third, nonionizing laser (150) or by using appropriately chirped laser pulses (151, 153). It has been concluded (150, 153) that the main difficulty in achieving efficient population transfer is related to the incoherent ionization channels, of which at least one is always present; these lead to inevitable irreversible population losses. It has been suggested (149, 150) that these losses can be reduced (although not eliminated) by choosing an appropriate region in the continuum where the ionization probability is minimal. It was shown later that incoherent ionization can be suppressed considerably by using a Fano-like resonance induced by an additional laser from a third state tuned near the region in the continuum where the incoherent ionization takes place; this leads to a significant increase in the transfer efficiency (154). Very recently, a similar scheme was proposed using a third laser, but tuned in the same region in the continuum as the pump and Stokes lasers, which provides an enhanced control of the population transfer (155). Finally, it has been suggested that a STIRAP-like process can take place also via an autoionizing state (156, 157).

3.3.3 Hyper-Raman STIRAP

3.3.3 Hyper-Raman STIRAP   The application of standard STIRAP to molecules, using two single-photon transitions (pump and Stokes), is often impeded by the fact that most molecules require ultraviolet or even vacuum ultraviolet pump photons to reach the first electronically excited states. (For the Stokes pulse, which connects the excited electronic state to a high vibrational level of the ground electronic state, optical wavelengths are usually sufficient.) It is difficult to provide vacuum ultraviolet pulses with adequate power and coherence properties. It is natural to consider achieving the pump excitation (and possibly the Stokes excitation too) by a two-photon transition. The corresponding $(2 + 1)$ and $(2 + 2)$ versions of STIRAP have been named hyper-Raman STIRAP (158–161). Although these extensions seem obvious, they turn out to be rather nontrivial.

The main obstacles in hyper-Raman STIRAP are the dynamic Stark shifts induced by the two-photon coupling. These Stark shifts, which are proportional to the laser intensities, modify the Bohr frequencies of the pump and Stokes transitions and destroy the multiphoton resonance between the initial and final states, which is crucial for the existence of the dark state. It has been found, both numerically and analytically, that high transfer efficiency in such a scheme can still be achieved by a suitable choice of static detunings of the carrier frequencies of the two pulses, which suppress the detrimental effect of the Stark shifts; these detuning ranges have been estimated analytically (159). It is interesting to note that, unlike the purely adiabatic evolution in STIRAP, successful population transfer in hyper-Raman STIRAP occurs as a result of a combination of adiabatic and diabatic time evolution, as in SCRAP (Section 2.2). Moreover, unlike STIRAP, the intermediate state does acquire some transient population; again, it can be reduced by suitable static detunings.

It should be pointed out that the Stark shifts are also nonzero in traditional STIRAP, but they are usually negligible compared with the one-photon on resonance couplings (given by the Autler-Townes splittings). In $(2 + 1)$-STIRAP the fundamental field (ω_P) is very strong, and the related Stark shift is usually not small compared with the two-photon coupling ($2\omega_P$).

3.3.4 Adiabatic Passage by Light-Induced Potentials

Recently, Garraway & Suominen (162) (see also 163, 164) have suggested, on the basis of numerical calculations for sodium dimers, that the STIRAP ideas of counterintuitively ordered laser pulses and adiabatic evolution can be applied to the transfer of a wave packet from one molecular potential to the displaced ground vibrational state of another. This process—termed adiabatic passage by light-induced potentials (APLIP)— seemingly violates the Frank-Condon principle because the overlap between the initial and final wavefunctions is very small (the two wavepackets were displaced at a distance seven times larger than their widths). There is, however, no such violation, because the time scale of the process is close to, but longer than, the vibrational time scale. APLIP shares many features with STIRAP, such as high efficiency and insensitivity to pulse parameters. However, in contrast to STIRAP, the two-photon resonance condition in APLIP cannot be satisfied (except at a certain time), and the main mechanism for the transfer of the wave packet is through a "valley" that emerges in the time-dependence of the light-induced potential, as shown in Figure 16 (*left*). Figure 16 (*right*) shows how the wavepacket gradually
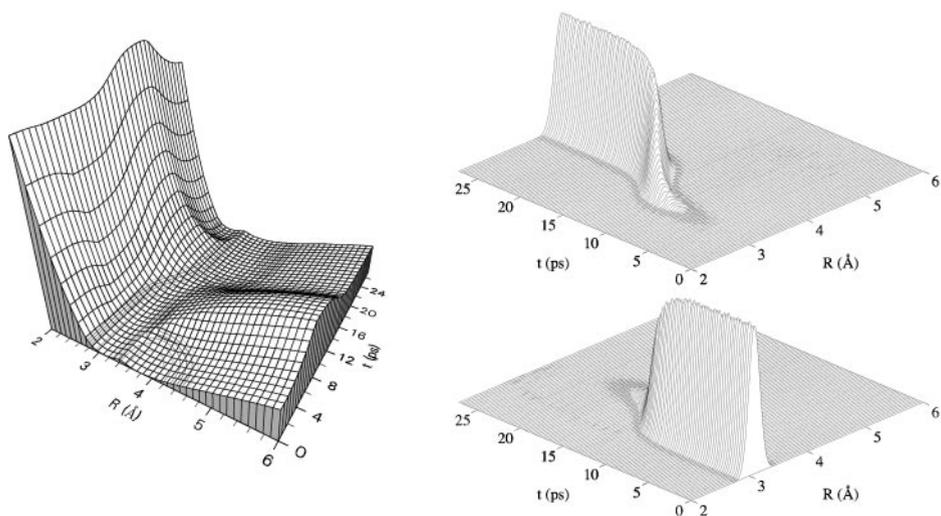
Figure 16 (*Left*) light-induced potential. The population flows through the "valley" in this potential. (*Right*) Time evolution of the ground-state (*lower*) and excited-state (*upper*) populations. Reprinted from (162) with permission.

disappears from the ground-state potential (lower plot) and appears in the excited-state one (upper plot). Although the original proposal assumed transitions between the lowest vibrational states ($v = v' = v'' = 0$), recent calculations (165) extended APLIP to excited vibrational states.

3.3.5 Creation of Coherent Superpositions by Modifications of STIRAP
STIRAP can be used not only to transfer population completely from one state to another, but also to create coherent superpositions of atomic or molecular states. The most obvious approach is to interrupt the time evolution of the dark state (21) at a certain intermediate time, when it is a superposition of the initial state ψ_1 and the final state ψ_3 (126, 166–168). Then only a fraction of the total population is transferred to ψ_3, and the composition of the superposition depends on the ratio between the pump and Stokes Rabi frequencies at the turn-off time. This fractional STIRAP has been demonstrated experimentally (167). A smooth realization of this scheme has also been proposed (169).

A more sophisticated variant of STIRAP has been proposed (170, 171) and demonstrated (172) in which the usual three-state STIRAP is supplied with an additional state ψ_4, coupled to the intermediate state ψ_2 by a third, control laser. Such a scheme (tripod-STIRAP) has two, rather than one, dark states. Because they are degenerate, transitions between them take place even in the adiabatic limit and eventually lead to the creation of a coherent superposition of ψ_1 and ψ_3. The composition of this superposition depends on, and therefore can be controlled by, the time delay between the pump and Stokes pulses and the strength of the control pulse.

3.4   Applications of Stimulated Raman Adiabatic Passage

3.4.1 Control of Chemical Reactions
The remarkable properties of STIRAP have already had applications in many diverse areas. The first implementation of STIRAP has been in a crossed-beam reactive scattering experiment (173). It allowed investigation of the effect of vibrational excitation on the cross section for the chemiluminescent channel in the process $Na_2(v) + Cl \rightarrow NaCl + Na^*$ in crossed particle beams. It was found that the cross sections increased by about 0.75% per vibrational level in the range $3 \leq v \leq 19$.

Another example is the detailed study of the reaction $Na_2(v'', j'') + H \rightarrow NaH(v', j') + Na$, where the angular distribution and the population distribution have been determined for the product molecule NaH for a range of selectively populated levels v'' of the reagent molecule Na_2 (174). STIRAP has also been used to investigate the dependence of the dissociative attachment process $Na_2(v'', j'') + e^- \rightarrow Na + Na^-$ (with electron energies <1 eV) on the vibrational excitation by exciting efficiently and very selectively the Na_2 molecules to a specific vibrationally excited level (175). The vibrational excitation up to $v'' = 12$ has increased the state-dependent dissociative attachment rate by more than three orders of magnitudes.

3.4.2 Atom Optics Coherent population transfer between atomic states is always accompanied by transfer of photon momenta to the atoms. Momentum transfer is the basis of atom optics, particularly in the design of its key elements—atom mirrors and beam splitters. Because STIRAP enables efficient, robust, and dissipation-free population transfer, it was soon realized that it is a perfect tool for coherent momentum transfer (126). A particularly appropriate system for momentum transfer is the multi-state chain formed from the magnetic sublevels of two degenerate levels, driven by two delayed laser pulses with opposite circular polarizations. An example in the case when $J_g = J_e = 2$, demonstrated in a recent experiment (90), is shown in Figure 17. A beam of metastable neon atoms, prepared by optical pumping into the $M = 2$ magnetic sublevel of the $^3P_2$ metastable level crossed two slightly displaced circularly polarized cw laser beams. The two beams were ordered counterintuitively, so that the atoms encountered the σ^+ beam (the Stokes) first and then the σ^- beam (the pump). In the adiabatic limit, the population was completely transferred to the $M = -2$ sublevel of the $^3P_2$ level, without residing at any time in the $M = -1$ and $M = 1$ sublevels of the decaying excited level $^3D_2$. Because the two laser beams propagated in opposite directions, the atom received a total momentum of $4\hbar k$ in the direction of the σ^- beam during its journey from the $M = 2$ sublevel to the $M = -2$ sublevel: $2\hbar k$ momentum owing to absorption of two photons from the σ^- beam (which transfer their momenta to the atom) and another momentum $2\hbar k$ in the same direction owing to recoil from the stimulated emission of two photons into the σ^+ beam. The experimental results in Figure 17 correspond to a double passage from the $M = 2$ sublevel to the $M = -2$ sublevel and then back to the $M = 2$ sublevel, resulting in the transfer of eight photon momenta.
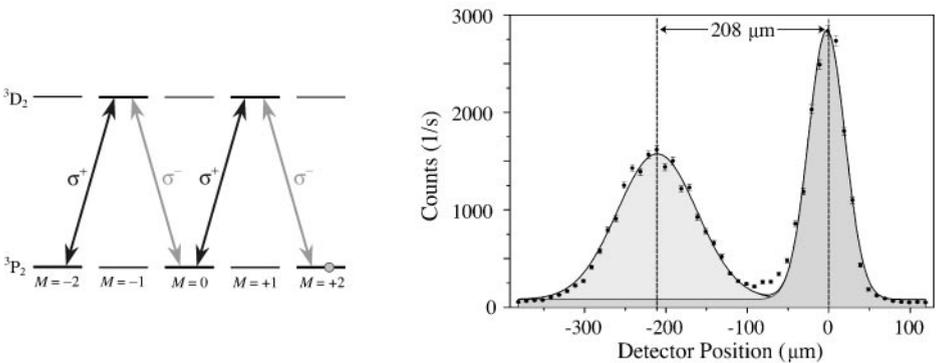

Figure 17 (*Left*) Linkage pattern between the Zeeman sublevels in the $^3P_2$-$^3D_2$ transition in Ne* driven by a pair of counterpropagating and displaced σ^+ and σ^- laser beams. (*Right*) Experimental results showing deflection of a beam of ^{20}Ne* atoms owing to transfer of eight photon momenta after double adiabatic passage from the $M = 2$ sublevel to $M = -2$ and then back to $M = 2$. The narrower, undeflected original distribution is observed owing to the presence of ^{22}Ne isotope atoms that are insensitive to light.

Coherent momentum transfer by adiabatic passage in similar chains of Zeeman sublevels has been demonstrated in a number of other experiments. Pillet et al (129, 130) and Goldner et al (131, 132) have reported momentum transfer of $8\hbar k$ resulting from the single-pass adiabatic passage between the $M_F = -4$ and $M_F = 4$ Zeeman sublevels in the hyperfine transition $F_g = 4 \leftrightarrow F_e = 4$ of the cesium D_2 line with 50% efficiency. Lawall & Prentiss (166) have demonstrated momentum transfer of $4\hbar k$ with 90% efficiency in the $2^3 S_1$-$2^3 P_0$ transition of He*, after double adiabatic passage ($M = -1 \rightarrow M = 1 \rightarrow M = -1$) between the ground-state sublevels. Chu et al (167, 168) have built the first atomic interferometer based on STIRAP in the transition between the two cesium hyperfine ground states ($6S_{1/2}$, $F = 3$, $M_F = 0$) and ($6S_{1/2}$, $F = 4$, $M_F = 0$) via the excited state ($6P_{1/2}$, $F = 3$ or 4, $M_F = 1$). They have achieved multiple-pass coherent transfer of more than 140 photon momenta with 95% efficiency per exchanged photon pair. Figure 18 shows the observed interference fringes. Burnett and co-workers (176–180) have also demonstrated coherent momentum transfer in cesium, both with beams having circular/circular and others having circular/linear polarizations. Finally, a multiple-beam atomic interferometer has been demonstrated wherein a beam of cesium atoms has been split into five spatially distinct beams (separated by two-photon momenta), corresponding to the magnetic sublevels $M = -4, -2, 0, 2, 4$, and then recombined (181).

3.4.3 Laser Cooling

The STIRAP technique has been successfully applied in laser-cooling experiments to coherently manipulate the atomic wave packets resulting from subrecoil laser cooling by velocity selective coherent population trapping (182–191). The momentum distribution of atoms cooled by velocity selective coherent population trapping has two peaks at $+\hbar k$ and $-\hbar k$, both with widths smaller than the photon recoil momentum $\hbar k$. Hänsch et al (192) have used adiabatic passage to coherently transfer rubidium atoms cooled by velocity selective coherent population trapping into a single momentum state, still with a subrecoil momentum spread. Kulin et al (193) have demonstrated adiabatic transfer of metastable helium atoms into a single wave packet or into two coherent wave packets, while retaining the subrecoil momentum dispersion of the initial wave packets. They have achieved nearly 100% transfer efficiency in one and two dimensions, and 75% in three dimensions, while being able to choose at will the momentum direction and the internal state of the atoms.

3.4.4 Measurement of Weak Magnetic Fields

The potential of STIRAP for atom beam deflection by coherent momentum transfer has been used to create a technique (called Larmor velocity filter) for measuring very small magnetic fields along the axis of the atomic beam (90). The scheme, which was demonstrated with metastable neon atoms, consisted of two STIRAP zones. In the first zone atoms were prepared in the $M = 2$ sublevel of the $^3 P_2$ metastable state and transferred to the $M = -2$ sublevel. They were transferred back to the initial $M = 2$ sublevel in the second zone provided they remained in the $M = -2$ state along the path
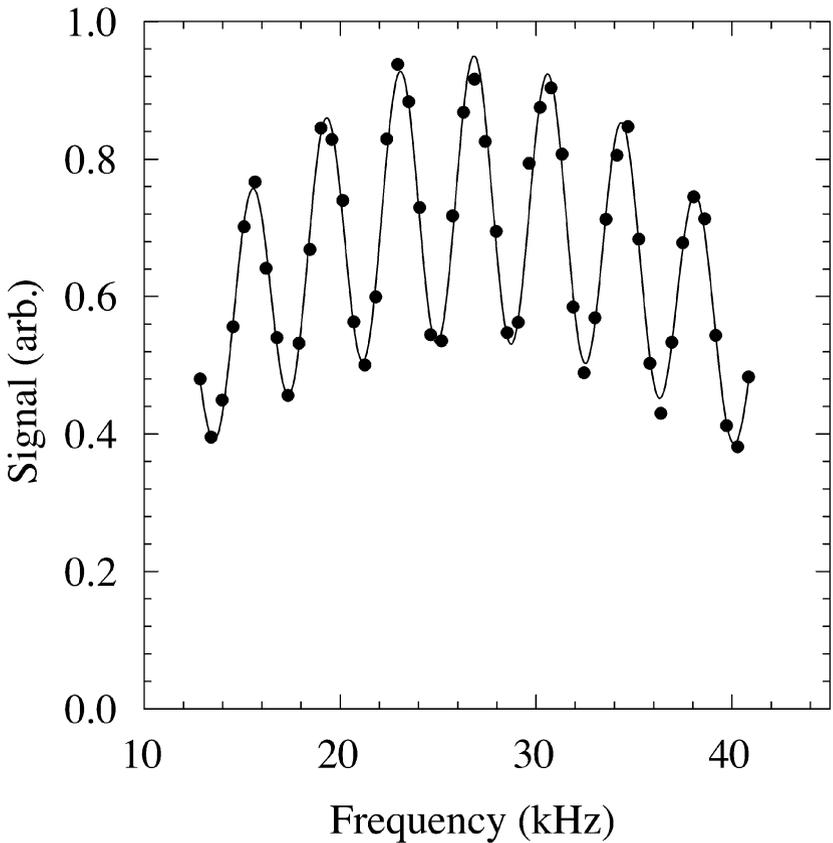
Figure 18 Interference fringes for an atomic interferometer based on adiabatic passage. The dots are experimental data and the curve is a fit by a cosine function with a Gaussian envelope. Reprinted from (167) with permission.

between the two zones (cf Figure 17). Larmor precession due to a magnetic field in the region between the two transfer zones mixed the magnetic sublevels and interfered with the momentum transfer. The resulting narrow-peaked pattern, an example of which is shown in Figure 19, allowed measurement of weak magnetic fields.

3.4.5 Cavity Quantum Electrodynamics The potential of STIRAP in cavity quantum electrodynamics has been pointed out by Kimble et al (194, 195) Parkins & Kimble (196). They proposed to use STIRAP to create coherent superpositions of photon-number states by strongly coupling an atom to a cavity field. Then the atomic ground-state Zeeman coherence (prepared by some preliminary excitation scheme) can be mapped to the cavity mode by adiabatic passage in
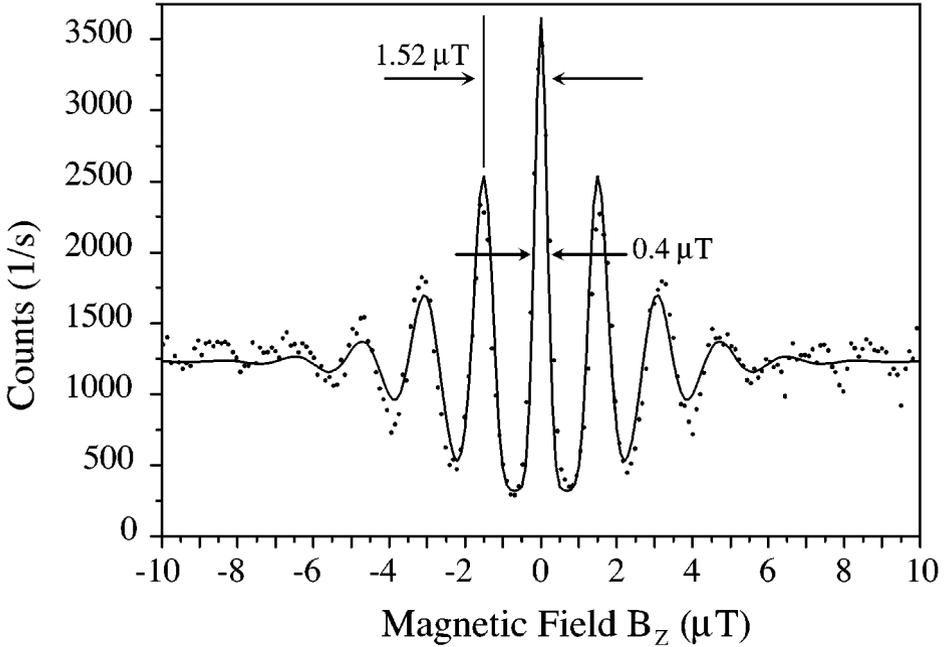
Figure 19 Variation of the flux of deflected Ne* atoms in the Larmor velocity filter with the magnetic field strength.

a decoherence-free fashion by a pair of two delayed laser pulses, one circularly and another linearly polarized. This idea was extended recently to the case of two degenerate cavity modes with orthogonal polarizations (197).

The above scheme is reversible and allows the opposite process, of mapping cavity-mode fields onto atomic ground-state Zeeman coherence. This mapping provides a possibility for measuring cavity fields (195). The atomic angular momentum state can be measured by the Newton-Young method (198) with a finite number of magnetic dipole measurements using Stern-Gerlach analyzers. Alternatively, the parameters of the atomic superposition can be measured by coupling this degenerate atomic state to an excited state by an elliptically polarized laser pulse and measuring the subsequent fluorescence (199, 200).

3.4.6 Bose-Einstein Condensation   It has been suggested recently, on the basis of numerical simulations (201–204), that STIRAP can be used to induce coherent two-color photo-association of a Bose-Einstein condensate in free-bound-bound transitions and convert an atomic condensate to a molecular one. It was concluded that Bose stimulation can enhance the atomic free-bound dipole matrix element to the extent enabling photo-associative STIRAP.

4.   CONCLUSIONS

Many contemporary fields in atomic, molecular, and optical physics require preparation of samples in which almost all of the population resides in a preselected excited state. Although a variety of methods have been proposed and tried over the years, many of the most successful are based on some application of adiabatic time evolution of the quantum system.

The theoretical description of such time dependence is most easily presented with the aid of adiabatic states: If the evolution is adiabatic then at all times the state vector remains aligned with one of these states. The experimenter has various guides for the applicability of adiabatic passage—the adiabatic conditions. Typically, these require that excitation pulses be strong and smooth and that the interaction act for a "long" time compared with a characteristic atomic time scale. Often this is expressed as the requirement that a time-integrated Rabi frequency be much larger than unity. What typically sets adiabatic techniques apart from other pulsed-excitation techniques is the relative insensitivity of the transfer efficiency to interaction parameters; adiabatic techniques are not sensitive to pulse area, for example.

In simplest form, adiabatic passage can completely invert the population of a two-state system using a level crossing. Numerous extensions have been devised and put to practical use. One very useful extension uses two sequential pulses to stimulate a Raman transition—the STIRAP technique. This too has been extended in a variety of ways from the initial demonstration involving three states. We have mentioned a number of these.

This review is primarily concerned with techniques for producing complete population transfer between two quantum states. There is also much contemporary interest in producing coherent superpositions of quantum states, sometimes using variants of the techniques discussed here to produce partial population transfer.

As laser technology continues to improve and experimenters acquire lasers with ever higher intensity and purer spectral content, one can expect to see imaginative new applications of adiabatic passage to the task of transferring populations between quantum states.

Visit the Annual Reviews home page at www.AnnualReviews.org

LITERATURE CITED

1. Einstein A. 1917. *Phys. Z.* 18:121. Translated, reprinted in van der Waerden. 1968. *Sources of Quantum Mechanics*. New York: Dover
2. Shore BW. 1990. *The Theory of Coherent Atomic Excitation*. New York: Wiley
3. Hamilton CE, Kinsey JL, Field RW. 1986. *Annu. Rev. Phys. Chem.* 37:493–524
4. Dai HL, Field RW. 1995. *Molecular Dynamics, Spectroscopy by Stimulated Emission Pumping*. Singapore: World Sci.
5. Messiah A. 1962. *Quantum Mechanics*. New York: North-Holland
6. Crisp MD. 1973. *Phys. Rev. A* 8:2128–35
7. Landau LD. 1932. *Phys. Z. Sowjetunion* 2:46
8. Zener C. 1932. *Proc. R. Soc. London Ser. A* 137:696
9. Allen L, Eberly JH. 1975. *Optical Resonance, Two-Level Atoms*. New York: Dover
10. Hioe FT. 1984. *Phys. Rev. A* 30:2100–3
11. Demkov YN, Kunike M. 1969. *Vestn. Leningr. Univ. Fiz. Khim.* 16:39–45
12. Suominen K-A, Garraway BM. 1992. *Phys. Rev. A* 45:374–86
13. Bloch F. 1946. *Phys. Rev.* 70:460–74
14. Abragam A. 1961. *The Principles of Nuclear Magnetism*. Oxford: Clarendon
15. Treacy EB. 1968. *Phys. Lett. A* 27:421
16. Loy MMT. 1974. *Phys. Rev. Lett.* 32:814–17
17. Grischkowsky D, Loy MMT. 1975. *Phys. Rev. A* 12:1117–20
18. Grischkowsky D, Loy MMT, Liao PF. 1975. *Phys. Rev. A* 12:2514–33
19. Grischkowsky D. 1976. *Phys. Rev. A* 14:802–12
20. Brewer RG, Hahn EL. 1975. *Phys. Rev. A* 11:1641–49
21. Loy MMT. 1976. *Phys. Rev. Lett.* 36:1454–57
22. Loy MMT. 1978. *Phys. Rev. Lett.* 41:473–76
23. Hamadani SM, Mattick AT, Kurnit NA, Javan A. 1975. *Appl. Phys. Lett.* 27:21–24
24. Avrillier S, Raimond J-M, Bordé CJ, Bassi D, Scoles G. 1981. *Opt. Commun.* 30:311
25. Adam AG, Gough TE, Isenor NR, Scoles G. 1985. *Phys. Rev. A* 32:1451–57
26. Leidenbaum C, Stolte S, Reuss J. 1989. *Phys. Rep.* 178:1–24
27. Kroon JPC, Senhorst HAJ, Beijerinck HCW, Verhaar BJ, Verster NF. 1985. *Phys. Rev. A* 31:3724–32
28. Lorent V, Claeys W, Cornet A, Urbain X. 1987. *Opt. Commun.* 64:41–44
29. Diels J-C, Rudolph W. 1996. *Ultrashort Laser Pulse Phenomena: Fundamentals, Techniques, Applications on a Femtosecond Time Scale*. San Diego: Academic
30. Chergui M. 1996. *Femtochemistry: Ultrafast Chemical, Physical Processes in Molecular Systems*. Singapore: World Sci.
31. Melinger JS, Hariharan A, Gandhi SR, Warren WS. 1991. *J. Chem. Phys.* 95:2210–13
32. Melinger JS, Gandhi SR, Hariharan A, Tull JX, Warren WS. 1992. *Phys. Rev. Lett.* 68:2000–3
33. Melinger JS, Gandhi SR, Hariharan A, Goswami D, Warren WS. 1994. *J. Chem. Phys.* 101:6439–54
34. Hillegas CW, Tull JX, Goswami D, Strickland D, Warren WS. 1994. *Opt. Lett.* 19:737–39
35. Weiner AM. 1995. *Prog. Quant. Electr.* 19:161–237

36. Dugan MA, Tull JX, Warren WS. 1997. *J. Opt. Soc. Am. B* 14:2348–58
37. Fetterman MR, Goswami D, Keusters D, Yang W, Rhee J-K, Warren WS. 1998. *Opt. Express* 3:366–75
38. Warren WS, Rabitz H, Dahleh M. 1993. *Science* 259:1581–89
39. Noordam LD, Joosen W, Broers B, ten Wolde A, Lagendijk A, et al. 1991. *Opt. Commun.* 85:331
40. Broers B, van Linden van den Heuvell HB, Noordam LD. 1992. *Phys. Rev. Lett.* 69:2062–65
41. Broers B, Noordam LD, van Linden van den Heuvell HB. 1992. *Phys. Rev. A* 46:2749–56
42. Broers B, van Linden van den Heuvell HB, Noordam LD. 1992. *Opt. Commun.* 91:57–61
43. Balling P, Maas DJ, Noordam LD. 1994. *Phys. Rev. A* 50:4276–85
44. Maas DJ, Rella CW, Antoine P, Toma ES, Noordam LD. 1999. *Phys. Rev. A* 59:1374–81
45. Vrijen RB, Lankhuijzen GM, Maas DJ, Noordam LD. 1996. *Comments At. Mol. Phys.* 33:67–82
46. Vrijen RB, Duncan DI, Noordam LD. 1997. *Phys. Rev. A* 56:2205–12
47. Maas DJ, Duncan DI, van der Meer AFG, van der Zande WJ, Noordam LD. 1997. *Chem. Phys. Lett.* 270:45–49
48. Maas DJ, Duncan DI, Vrijen RB, van der Zande WJ, Noordam LD. 1998. *Chem. Phys. Lett.* 290:75–80
49. Maas DJ, Vrakking MJJ, Noordam LD. 1999. *Phys. Rev. A* 60:1351–62
50. Goswami D, Warren WS. 1994. *Phys. Rev. A* 50:5190–96
51. Herrmann J, Mondry J. 1988. *J. Mod. Opt.* 35:1919–32
52. Yatsenko LP, Shore BW, Halfmann T, Bergmann K, Vardi A. 1999. *Phys. Rev. A* 60:R4237–40
53. Rickes T, Yatsenko LP, Steuerwald S, Halfmann T, Shore BW, et al. 2000. *J. Chem. Phys.* 113:534–46
54. Hioe FT. 1983. *Phys. Lett. A* 99:150
55. Hioe FT, Eberly JH. 1984. *Phys. Rev. A* 29:1164–67
56. Oreg J, Hioe FT, Eberly JH. 1984. *Phys. Rev. A* 29:690–97
57. Oreg J, Hazak G, Eberly JH. 1985. *Phys. Rev. A* 32:2776–83
58. Solá IR, Malinovsky VS, Chang BY, Santamaria J, Bergmann K. 1999. *Phys. Rev. A* 59:4494–501
59. Chelkowski S, Bandrauk AD, Corkum PB. 1990. *Phys. Rev. Lett.* 65:2355–58
60. Chelkowski S, Bandrauk AD. 1991. *Chem. Phys. Lett.* 186:264–69
61. Chelkowski S, Bandrauk AD. 1993. *J. Chem. Phys.* 99:4279–87
62. Melinger JS, McMorrow D, Hillegas C, Warren WS. 1995. *Phys. Rev. A* 51:3366–69
63. Guérin S. 1997. *Phys. Rev. A* 56:1458–62
64. Ghosh S, Sen S, Bhattacharyya SS, Saha S. 1999. *Phys. Rev. A* 59:4475–84
65. Chelkowski S, Gibson GN. 1995. *Phys. Rev. A* 52:R3417–20
66. Chelkowski S, Bandrauk AD. 1997. *J. Raman Spectr.* 28:459–66
67. Davis JC, Warren WS. 1999. *J. Chem. Phys.* 110:4229–42
68. Karczmarek J, Wright J, Corkum P, Ivanov M. 1999. *Phys. Rev. Lett.* 82:3420–23
69. Villeneuve DM, Aseyev SA, Dietrich P, Spanner M, Ivanov MY, Corkum PB. 2000. *Phys. Rev. Lett.* 85:542–45
70. Demkov YN, Osherov VI. 1968. *Sov. Phys. JETP* 26:916–21
71. Demkov YN, Ostrovsky VN. 1995. *J. Phys. B* 28:403–14
72. Carroll CE, Hioe FT. 1985. *J. Opt. Soc. Am. B* 2:1355–60
73. Carroll CE, Hioe FT. 1986. *J. Phys. A* 19:1151–61
74. Carroll CE, Hioe FT. 1986. *J. Phys. A* 19:2061–73
75. Brundobler S, Elser V. 1993. *J. Phys. A* 26:1211–27
76. Harmin DA. 1991. *Phys. Rev. A* 44:433–61

77. Ostrovsky VN, Nakamura H. 1997. *J. Phys. A* 30:6939–50

78. Mewes M-O, rews MR, Kurn DM, Durfee DS, Townsend CG, Ketterle W. 1997. *Phys. Rev. Lett.* 78:582–85

79. Vitanov NV, Suominen K-A. 1997. *Phys. Rev. A* 56:R4377–80

80. Kuklinski JR, Gaubatz U, Hioe FT, Bergmann K. 1989. *Phys. Rev. A* 40:6741–44

81. Gaubatz U, Rudecki P, Schiemann S, Bergmann K. 1990. *J. Chem. Phys.* 92:5363–76

82. Bergmann K, Shore BW. 1995. *Coherent Population Transfer*, See Ref. 4, pp. 315–73

83. Shore BW. 1995. *Contemp. Phys.* 36:15–28

84. Bergmann K, Theuer H, Shore BW. 1998. *Rev. Mod. Phys.* 70:1003–25

85. Alzetta G, Gozzini A, Moi L, Orriols G. 1976. *Nuovo Cim. B* 36:5–20

86. Alzetta G, Moi L, Orriols G. 1979. *Nuovo Cim. B* 52:2333–46

87. Arimondo E, Orriols G. 1976. *Lett. Nuovo Cim.* 17:333–38

88. Arimondo E. 1996. In *Progress in Optics*, Vol. XXXV, ed. E Wolf, pp. 259–356. Amsterdam: North-Holland

89. Gray HR, Whitley RM, Stroud CR. 1978. *Opt. Lett.* 3:218–20

90. Theuer H, Bergmann K. 1998. *Eur. Phys. J. D* 2:279–89

91. He G-Z, Kuhn A, Schiemann S, Bergmann K. 1990. *J. Opt. Soc. Am. B* 7:1960–69

92. Shore BW, Bergmann K, Kuhn A, Schiemann S, Oreg J, Eberly JH. 1992. *Phys. Rev. A* 45:5297–300

93. Shore BW, Bergmann K, Oreg J. 1992. *Z. Phys. D* 23:33–39

94. Vitanov NV, Stenholm S. 1997. *Phys. Rev. A* 55:648–60

95. Laine TA, Stenholm S. 1996. *Phys. Rev. A* 53:2501–12

96. Vitanov NV, Stenholm S. 1996. *Opt. Commun.* 127:215–22

97. Elk M. 1995. *Phys. Rev. A* 52:4017–22

98. Drese K, Holthaus M. 1998. *Eur. Phys. J. D* 3:73–86

99. Fleischhauer M, Manka AS. 1996. *Phys. Rev. A* 54:794–803

100. Fleischhauer M, Unanyan R, Shore BW, Bergmann K. 1999. *Phys. Rev. A* 59:3751–60

101. Kobrak MN, Rice SA. 1998. *Phys. Rev. A* 57:1158–63

102. Vitanov NV, Stenholm S. 1997. *Opt. Commun.* 135:394–405

103. Danileiko MV, Romanenko VI, Yatsenko LP. 1994. *Opt. Commun.* 109:462–66

104. Romanenko VI, Yatsenko LP. 1997. *Opt. Commun.* 140:231–36

105. Fewell MP, Shore BW, Bergmann K. 1997. *Aust. J. Phys.* 50:281–304

106. Band YB, Julienne PS. 1991. *J. Chem. Phys.* 94:5291–98

107. Vitanov NV, Stenholm S. 1997. *Phys. Rev. A* 56:1463–71

108. Glushko B, Kryzhanovsky B. 1992. *Phys. Rev. A* 46:2823–30

109. Coulston GW, Bergmann K. 1992. *J. Chem. Phys.* 96:3467–95

110. Vitanov NV, Stenholm S. 1999. *Phys. Rev. A* 60:3820–32

111. Band YB, Magnes O. 1994. *Phys. Rev. A* 50:584–94

112. Kobrak MN, Rice SA. 1998. *Phys. Rev. A* 58:2885–94

113. Unanyan R, Guérin S, Shore BW, Bergmann K. 2000. *Eur. Phys. J. D* 8:443–49

114. Gaubatz U, Rudecki P, Becker M, Schiemann S, Külz M, Bergmann K. 1988. *Chem. Phys. Lett.* 149:463–68

115. Rubahn H-G, Konz E, Schiemann S, Bergmann K. 1991. *Z. Phys. D* 22:401–6

116. Lindinger A, Verbeek M, Rubahn H-G. 1997. *Z. Phys. D* 39:93–100

117. Kuhn A, Coulston G, He G-Z, Schiemann S, Bergmann K, Warren WS. 1992. *J. Chem. Phys.* 96:4215–23

118. Schiemann S, Kuhn A, Steuerwald S,

Bergmann K. 1993. *Phys. Rev. Lett.* 71:3637–40

119. Kuhn A, Steuerwald S, Bergmann K. 1998. *Eur. Phys. J. D* 1:57–70

120. Halfmann T, Bergmann K. 1996. *J. Chem. Phys.* 104:7068–72

121. Süptitz W, Duncan BC, Gould PL. 1997. *J. Opt. Soc. Am. B* 14:1001–8

122. Shore BW, Martin J, Fewell MP, Bergmann K. 1995. *Phys. Rev. A* 52:566–82

123. Martin J, Shore BW, Bergmann K. 1995. *Phys. Rev. A* 52:583–93

124. Martin J, Shore BW, Bergmann K. 1996. *Phys. Rev. A* 54:1556–69

125. Shore BW, Bergmann K, Oreg J, Rosenwaks S. 1991. *Phys. Rev. A* 44:7442–47

126. Marte P, Zoller P, Hall JL. 1991. *Phys. Rev. A* 44:4118–21

127. Smith AV. 1992. *J. Opt. Soc. Am. B* 9:1543–51

128. Oreg J, Bergmann K, Shore BW, Rosenwaks S. 1992. *Phys. Rev. A* 45:4888–96

129. Pillet P, Valentin C, Yuan R-L, Yu J. 1993. *Phys. Rev. A* 48:845–48

130. Valentin C, Yu J, Pillet P. 1994. *J. Phys. II* 4:1925–37

131. Goldner LS, Gerz C, Spreeuw RJC, Rolston SL, Westbrook CI, et al. 1994. *Phys. Rev. Lett.* 72:997–1000

132. Goldner LS, Gerz C, Spreeuw RJC, Rolston SL, Westbrook CI, et al. 1994. *Quantum Opt.* 6:387–89

133. Malinovsky VS, Tannor DJ. 1997. *Phys. Rev. A* 56:4929–37

134. Vitanov NV. 1998. *Phys. Rev. A* 58:2295–309

135. Vitanov NV, Shore BW, Bergmann K. 1998. *Eur. Phys. J. D* 4:15–29

136. Nakajima T. 1999. *Phys. Rev. A* 59:559–68

137. Morris JR, Shore BW. 1983. *Phys. Rev. A* 27:906–12

138. Hioe FT, Carroll CE. 1988. *Phys. Rev. A* 37:3000–5

139. Band YB, Julienne PS. 1991. *J. Chem. Phys.* 95:5681–85

140. Carroll CE, Hioe FT. 1992. *Phys. Rev. Lett.* 68:3523–26

141. Carroll CE, Hioe FT. 1993. *Phys. Rev. A* 47:571–80

142. Knight PL. 1984. *Comments At. Mol. Phys.* 15:193–214

143. Knight PL, Lauder MA, Dalton BJ. 1990. *Phys. Rep.* 190:1–61

144. Halfmann T, Yatsenko LP, Shapiro M, Shore BW, Bergmann K. 1998. *Phys. Rev. A* 58:R46–49

145. Yatsenko LP, Halfmann T, Shore BW, Bergmann K. 1999. *Phys. Rev. A* 59:2926–47

146. Nakajima T, Elk M, Zhang J, Lambropoulos P. 1994. *Phys. Rev. A* 50:R913–16

147. Fano U. 1961. *Phys. Rev.* 124:1866–78

148. Carroll CE, Hioe FT. 1995. *Phys. Lett. A* 199:145–50

149. Carroll CE, Hioe FT. 1996. *Phys. Rev. A* 54:5147–51

150. Yatsenko LP, Unanyan RG, Bergmann K, Halfmann T, Shore BW. 1997. *Opt. Commun.* 135:406–12

151. Paspalakis E, Protopapas M, Knight PL. 1997. *Opt. Commun.* 142:34–40

152. Paspalakis E, Protopapas M, Knight PL. 1998. *J. Phys. B* 31:775–94

153. Vitanov NV, Stenholm S. 1997. *Phys. Rev. A* 56:741–47

154. Unanyan RG, Vitanov NV, Stenholm S. 1998. *Phys. Rev. A* 57:462–66

155. Unanyan RG, Vitanov NV, Shore BW, Bergmann K. 2000. *Phys. Rev. A* 61:043408

156. Nakajima T, Lambropoulos P. 1996. *Z. Phys. D* 36:17–22

157. Paspalakis E, Knight PL. 1998. *J. Phys. B* 31:2753–67

158. Yatsenko LP, Guérin S, Halfmann T, Boehmer K, Shore BW, Bergmann K. 1998. *Phys. Rev. A* 58:4683–90

159. Guérin S, Yatsenko LP, Halfmann T, Shore BW, Bergmann K. 1998. *Phys. Rev. A* 58:4691–704

160. Guérin S, Jauslin HR. 1998. *Eur. Phys. J. D* 2:99–113

161. Guérin S, Jauslin HR, Unanyan RG, Yatsenko LP. 1999. *Opt. Express* 4:84–90

162. Garraway BM, Suominen K-A. 1998. *Phys. Rev. Lett.* 80:932–35

163. Kallush S, Band YB. 2000. *Phys. Rev. A* 61:041401

164. Solá IR, Santamaría J, Malinovsky VS. 2000. *Phys. Rev. A* 61:043413

165. Rodriguez M, Garraway BM, Suominen K-A. 2000. *Phys. Rev. A* 62:053413

166. Lawall J, Prentiss M. 1994. *Phys. Rev. Lett.* 72:993–96

167. Weitz M, Young BC, Chu S. 1994. *Phys. Rev. Lett.* 73:2563–66

168. Weitz M, Young BC, Chu S. 1994. *Phys. Rev. A* 50:2438–44

169. Vitanov NV, Suominen K-A, Shore BW. 1999. *J. Phys. B* 32:4535–46

170. Unanyan R, Fleischhauer M, Shore BW, Bergmann K. 1998. *Opt. Commun.* 155:144–54

171. Unanyan RG, Shore BW, Bergmann K. 1999. *Phys. Rev. A* 59:2910–19

172. Theuer H, Unanyan RG, Habscheid C, Klein K, Bergmann K. 1999. *Opt. Express* 4:77–83

173. Dittmann P, Pesl FP, Martin J, Coulston GW, He G-Z, Bergmann K. 1992. *J. Chem. Phys.* 97:9472–75

174. Pesl FP, Lutz S, Bergmann K. 2001. In press

175. Külz M, Keil M, Kortyna A, Schellhaass B, Hauck J, Bergmann K, et al. 1996. *Phys. Rev. A* 53:3324–34

176. Featonby PD, Summy GS, Martin JL, Wu H, Zetie KP, et al. 1996. *Phys. Rev. A* 53:373–80

177. Featonby PD, Summy GS, Webb CL, Godun RM, Oberthaler MK, et al. 1998. *Phys. Rev. Lett.* 81:495–99

178. Morigi G, Featonby P, Summy G, Foot C. 1996. *Quant. Semiclass. Opt.* 8:641–53

179. Godun RM, Webb CL, Oberthaler MK, Summy GS, Burnett K. 1999. *Phys. Rev. A* 59:3775–81

180. Webb CL, Godun RM, Summy GS, Oberthaler MK, Featonby PD, et al. 1999. *Phys. Rev. A* 60:R1783–86

181. Weitz M, Heupel T, Hänsch TW. 1996. *Phys. Rev. Lett.* 77:2356–59

182. Aspect A, Armindo E, Kaiser R, Vanteenkiste N, Cohen-Tannoudji C. 1988. *Phys. Rev. Lett.* 61:826–29

183. Aspect A, Armindo E, Kaiser R, Vanteenkiste N, Cohen-Tannoudji C. 1989. *J. Opt. Soc. Am. B* 6:2112–24

184. Chu S. 1998. *Rev. Mod. Phys.* 70:685–706

185. Cohen-Tannoudji CN. 1998. *Rev. Mod. Phys.* 70:707–20

186. Phillips WD. 1998. *Rev. Mod. Phys.* 70:721–42

187. Lawall J, Bardou F, Saubaméa B, Shimizu K, Leduc M, et al. 1994. *Phys. Rev. Lett.* 73:1915–18

188. Lawall J, Kulin S, Saubaméa B, Bigelow N, Leduc M, Cohen-Tannoudji C. 1995. *Phys. Rev. Lett.* 75:4194–97

189. Lawall J, Kulin S, Saubaméa B, Bigelow N, Leduc M, Cohen-Tannoudji C. 1996. *Laser Phys.* 6:153–58

190. Kasevich M, Weiss DS, Riis E, Moler K, Kasapi S, Chu S. 1991. *Phys. Rev. Lett.* 66:2297–300

191. Kasevich M, Chu S. 1992. *Phys. Rev. Lett.* 69:1741–44

192. Esslinger T, Sander F, Weidemüller M, Hemmerich A, Hänsch TW. 1996. *Phys. Rev. Lett.* 76:2432–35

193. Kulin S, Saubaméa B, Peik E, Lawall J, Hijmans TW, et al. 1997. *Phys. Rev. Lett.* 78:4185–88

194. Parkins AS, Marte P, Zoller P, Kimble HJ. 1993. *Phys. Rev. Lett.* 71:3095–98

195. Parkins AS, Marte P, Zoller P, Carnal O, Kimble HJ. 1995. *Phys. Rev. A* 51:1578–96

196. Parkins AS, Kimble HJ. 1999. *J. Opt. B* 1:496–504

197. Lange W, Kimble HJ. 2000. *Phys. Rev. A* 61:063817

198. Newton RG, Young B-L. 1968. *Ann. Phys.* 49:393–402

199. Vitanov NV, Shore BW, Unanyan RG,

Bergmann K. 2000. *Opt. Commun.* 179: 73–83

200. Vitanov NV. 2000. *J. Phys. B* 33:2333–46

201. Javanainen J, Mackie M. 1998. *Phys. Rev. A* 58:R789–92

202. Javanainen J, Mackie M. 1999. *Phys. Rev. A* 59:R3186–89

203. Mackie M, Javanainen J. 1999. *Phys. Rev. A* 60:3174–87

204. Mackie M, Kowalski R, Javanainen J. 2000. *Phys. Rev. Lett.* 84:3803–6